Constraints and Relations in Driven and Active Diffusions

by

Qi Gao

A dissertation submitted in partial fulfillment
of the requirements for the degree of
Doctor of Philosophy
(Physics)
in the University of Michigan
2023

Doctoral Committee:

Professor Jordan Horowitz, Chair
Professor Xiaoming Mao
Professor Mark Newman
Professor Kai Sun
Professor Qiong Yang

Qi Gao
convex@umich.edu
ORCID iD: 0000-0003-0489-2061

DEDICATION

To my parents.

ACKNOWLEDGEMENTS

My greatest gratitude goes to my awesome PhD advisor Jordan Horowitz for his sharp insights and kind guidance in my research. Jordan also patiently taught me his aesthetic, elegant presentation skills by going through all of my presentations slide by slide, for which I feel deeply grateful and fortunate. I am honored to join the Horowitz Lab as the first member and I am thankful for all the members for the supportive, professional and friendly atmosphere. I would like to thank Dr. Hyun-Myung Chun, for his solid work and tremendous, selfless help during our collaborations. I also want to thank Freddy Cisneros, Gabriela Fernandes Martins for all their genuine help during my research and presentations in the past years, and Dr. Sean Fancher for his help with my presentation. I want to thank Liz Tidwell, Andres Felipe Gonzalez Duran, Ally Murray and Harsha Gouda from the Dissertation Writing Group for their feedback on my thesis.

I would like to thank my faculty mentor, Prof. Xiaoming Mao for her nice lecturing in statistical physics and written recommendation. I want to thank Prof. Kai Sun for his lecturing and considerate, genuine advice in our correspondence. I am also very appreciative of Prof. Dieter Jaksch and Dr. Michael Lubasch for their sincere guidance, advice and recommendation prior to my PhD career. I will always be grateful and pay tribute to Prof. Charles Doering, for introducing me to the Horowitz group. I am truly thankful for Prof. Vanessa Sih for her kind help with the logistics in my PhD career and for the professional and cordial support from Lauren Segall, Tammy Kennedy, Cory Steiner, Jessie Presley and all the university support teams. Their impressive work brings sunshine to the PhD program.

As an international student far-from-home, my gratitude extends to my friends at Woodbury Gardens for making our house a home, especially during the pandemic. Thank you Jiaqi Shen, Jiayu Zhang for the delicacies and memories. Thank you Yiming Gong for sharing medicine and stories. Thank you Jiongsheng Cai, Heting Fu, Duoduo Wang, Binglin Song, Zhijian Hu, Alisher Duspayev and Nizar Ezroura for all the good times we spent together. Your friendship makes my graduate school an invaluable memory.

Finally I have to thank you mom and dad for your selfless unconditional love.

TABLE OF CONTENTS

LIST OF FIGURES

FIGURE

LIST OF ACRONYMS

TLA Three Letter Acronym

NESS Nonequilibrium Steady State

FDT Fluctuation Dissipation Theorem

FDR Fluctuation Dissipation Relation

FPE Fokker-Planck Equation

ABP Active Brownian Particles

OU Ornstein-Uhlenbeck

MTT Matrix Tree Theorem

ABSTRACT

In near-equilibrium thermodynamic systems, the fluctuation-dissipation theorem characterizes the responses of arbitrary observables due to small perturbations in terms of experimentally measurable equilibrium correlation functions. However, in far-from-equilibrium systems, the fluctuation-dissipation theorem is no longer valid and the approach to re-establishing the connection between the responses and correlations for nonequilibrium steady states requires detailed knowledge of the system's microscopic dynamics, which is usually prohibitively difficult to obtain.

This dissertation proposes a new perspective on studying nonequilibrium static responses in any system that can be modeled as a diffusion process with periodic boundary conditions. For one-dimensional diffusion processes I analyze the static response to perturbations of nonequilibrium steady state and demonstrate that an arbitrary perturbation can be broken up into a combination of three specific classes of perturbations that can be fruitfully addressed individually. For each class I derive a simple formula that quantitatively characterizes the response in terms of the strength of nonequilibrium driving valid arbitrarily far from equilibrium. Among the three classes of perturbations, I show that the perturbation in mobility has an important physical meaning of violation of the fluctuation-dissipation theorem. This motivates us to generalize the study in mobility perturbation for higher dimensions. I present the general Fourier expansion approach that can be used for studying this problem and the challenges for a general model. Then I show for several special cases some analytical or numerical bounds for mobility perturbation responses. Finally, for active Brownian particles, an application of studying the response in hydrodynamics gives the nonequilibrium Green-Kubo relations. This nonequilibrium Green-Kubo relation is numerically verified using molecular dynamics simulations and data analysis.

CHAPTER 1

Introduction and Theoretical Background

1.1 Introduction

Manipulating a physical system and observing its response is one of the most important approaches to understanding its properties. For example, we know a spring is stiff if when we pull it and it barely stretches; we know a liquid is viscous if when we pour it and it barely flows. Response quantifies how a system reacts to external stimuli and is thus considered as one of the basic properties of a physical system. Numerous physical quantities or concepts people studied in various fields can actually be viewed as related to the response, including the conductivity, the friction coefficient, the elastic modulus, the Green's function, the biochemical sensitivity, etc. For static or lifeless systems, which are at equilibrium, we have a well-established theoretical framework to study the responses, and the cornerstone of that framework is the fluctuation-dissipation theorem [1]. This theorem relates the responses, which are very challenging to measure directly in microscopic systems, to experimentally accessible quantities, the correlations. The significance of the fluctuation-dissipation theorem extends as the statistical-mechanical foundation of hydrodynamics, establishing Green-Kubo relations [2, 3], and as the theoretical scaffolding for cross-disciplinary experiments in statistical physics and biophysics, including light scattering and microrheology experiments [4].

Due to the early success of the equilibrium FDT, it is customary now to probe a system's behavior, no matter how far from equilibrium, in terms of responses to perturbations and correlation

functions too [5, 6, 7, 8, 9, 10, 11, 12, 13, 14]. In principle, the nonequilibrium responses indeed can generally be related to correlation functions [15]. It turns out that if we choose the observable involved in the correlation function to be conjugated to the external force with respect to the "potential" corresponding to the nonequilibrium steady state (NESS) probability distribution [16], we can get the FDT that is identical to the equilibrium case. Since the NESS probability distribution is typically unknown, it is difficult to directly use the nonequilibrium FDT except for simple single particle systems.

A complementary approach has been to characterize violations of the equilibrium-version of the FDT. Effective temperature [17, 18, 19] has been introduced to quantify the violation of the equilibrium FDT. Besides, the Harada-Sasa equality [20, 21] relates the violation of equilibrium FDT to the steady state energy dissipation rate for Brownian particles.

Instead of the exact formula of the nonequilibrium FDT, it is sometimes more convenient to use the bounds on the fluctuations or dissipations. Recent research reveals that there generally exist thermodynamic bounds on the fluctuations and responses. For systems that can be described by Markovian stochastic process, the relative fluctuations in generalized currents are bounded from below by the total dissipation rate, known as the thermodynamic uncertainty relations (TUR) [22, 23, 24]. Those bounds are expected to provide insight into nanotechnological devices because in the nano-scale systems, the number of atoms or molecules is small enough so the fluctuations play an important role. For example, the TUR can be used to bound the entropy production rate using statistical fluctuations in the probability currents [25]. It can also be used for estimating the upper limit of the efficiency of a processive molecule motor which is designed to pull cargo against a mechanical force or torque by consuming chemical work provided by ATP [26]. Since the response is related to the fluctuations by the FDT, the bounds on the response would suggest the design principles for high-sensitivity but low-noise devices [27].

Motivated by such ideas, it was recently found [27] that the magnitude of generic static responses for the finite state Markovian process are bounded from above by quantities that depend on the type of the response and the degree of the nonequilibrium driving.

An application of studying the response in hydrodynamics is the derivation of the nonequilibrium Green-Kubo relations. The recent work in [28] demonstrates that generally Green-Kubo relations for macroscopic transport coefficients maintain their equilibrium form arbitrarily far from equilibrium by introducing a class of perturbations with explicit conjugate variables whose response is given by simple nonequilibrium correlation functions, akin to the equilibrium FDT. An exploitation of this equilibrium-like fluctuation-response equality provides a theoretical foundation for linearized hydrodynamic equations governing transport in homogeneous nonequilibrium fluids.

In the following sections, I review some of the basic mathematics and important results in stochastic thermodynamics that serve as the theoretical background of the main results in this thesis. The basics presented here are adapted from the original forms to increase readability but should be easily generalized to more general forms.

1.2 Linear Response

In physical systems, response is usually manifested as the change in the average of some observable $\langle Q \rangle$ relative to the perturbation λ. For example, in a circuit we can apply a voltage as the perturbation and the relative response in electric current, as an observable, is the conductivity. In this thesis we only consider the case where the perturbation is small and thus the value of the perturbed observable can be approximately written as the unperturbed value plus the response term that is linear in the perturbation. The approach to study such response is known as linear response theory [29]. Now consider an equilibrium system with some number of mesoscopic states x under the small perturbation $\lambda(t)$ depending on time t. For simplicity we can assume x is discrete. Suppose the energy of the state x, U_x is under the influence of λ so that

$$U_x(\lambda) = U_x(0) - \lambda V_x, \tag{1.1}$$

where V_x is the a given function of x and is known as the conjugate variable of λ to the energy.

We use $\langle \ldots \rangle_0$ to denote the average in the unperturbed case and $\langle \ldots \rangle_\lambda$ for the average when perturbation λ is present. We want to evaluate the average value $\langle Q(t) \rangle_\lambda$ of observable Q at time t as a function of perturbation λ,

$$\langle Q(t) \rangle_\lambda = \sum_x Q_x(t) p_x(t; \lambda), \tag{1.2}$$

where $p_x(t; \lambda)$ is the probability distribution of the states at time t with perturbation λ present. To define the linear response we expand $\langle Q(t) \rangle_\lambda$ as a functional power series in λ

$$\langle Q(t) \rangle_\lambda = \langle Q(t) \rangle_0 + \int_{-\infty}^{+\infty} R_{Q,V}(t, s) \lambda(s) ds + o(\lambda), \tag{1.3}$$

where $R_{Q,V}(t, s)$ is known as the linear response function. This function must be zero when $t < s$ due to causality. Besides, it must be invariant under time translation

$$R_{Q,V}(t, s) = R_{Q,V}(t - s). \tag{1.4}$$

due to the homogeneity in time. The core of the linear response theory is to express this linear response function as equilibrium correlation, which is the equilibrium FDT we will introduce in the next section.

1.3 Equilibrium FDT

In this section we continue the study of linear response in section 1.2 and derive the equilibrium FDT. The derivation is adapted from [29].

Consider a perturbation scheme $\lambda(t) = \lambda^{(0)} \Theta(-t) e^{\epsilon t}$ where $\epsilon > 0$ is arbitrarily small and $\Theta(t)$ is the heaviside function. Such perturbation grows from zero since $t = -\infty$ to a small constant value $\lambda^{(0)}$ at time $t = 0$ and then is switched off at $t = 0$, as is shown in Fig. 1.1. Since ϵ is small, the system is always at equilibrium for $t \leq 0$. At $t = 0$ the probability distribution is

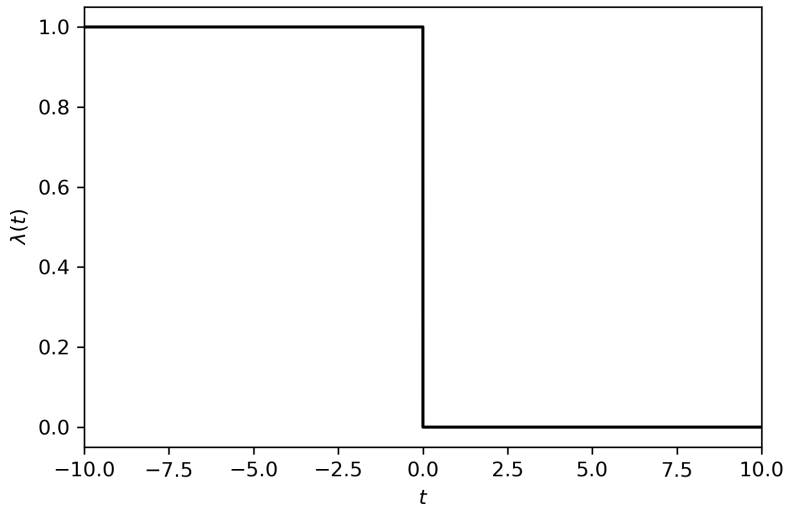

Figure 1.1: Illustration of perturbation scheme $\lambda(t) = \lambda^{(0)}\Theta(-t)e^{\epsilon t}$ with $\epsilon \to 0$ and $\lambda^{(0)}$. Such perturbation is essentially just $\Theta(-t)$.

the equilibrium distribution in the presence of constant perturbation $\lambda^{(0)}$, which is a Boltzmann distribution. The reason we consider such perturbation scheme is that we can guarantee the system is already at equilibrium for $t = 0$ so that the dynamics of $p_x(t;\lambda)$ is the same as one that satisfies the unperturbed dynamics, but with initial condition $p_x^{\text{eq}}(\lambda)$ which can be evaluated.

We assume $p_x(t;\lambda)$ can be evaluate as

$$p_x(t;\lambda) = \sum_y G_{xy}(t)p_y(0;\lambda) \tag{1.5}$$

where $G_{xy}(t)$ is the conditional probability of the system being in state x at time t given that it is in state y at time 0.

Since the perturbation is in the energy, we can express the perturbed equilibrium distribution $p_x^{\text{eq}}(\lambda)$ using the unperturbed probability distribution

$$p_x(0;\lambda) = p_x^{\text{eq}}(\lambda) = \frac{1}{N(\lambda^{(0)})}e^{-[U_x(0)-\lambda^{(0)}V_x]/k_BT} \tag{1.6}$$

where

$$N(\lambda^{(0)}) = \sum_x e^{-[U_x(0)-\lambda^{(0)}V_x]/k_BT} \tag{1.7}$$

is the normalization. Note that

$$\frac{\partial N(\lambda^{(0)})}{\partial \lambda^{(0)}}\Big|_{\lambda^{(0)}=0} = \sum_x \frac{V_x}{k_BT} e^{-U_x(0)/k_BT} = \frac{\langle V\rangle_0}{k_BT} N(\lambda^{(0)}), \tag{1.8}$$

where $\langle V\rangle_0$ is the equilibrium average of observable V in the absence of the perturbation. We want to expand $p_x(0;\lambda)$ in (1.6), which requires evaluating the derivative of $p_x(0;\lambda)$ in λ at $\lambda = 0$,

$$\frac{\partial p_x(0;\lambda)}{\partial \lambda^{(0)}}\Big|_{\lambda^{(0)}=0} = (V_x - \langle V\rangle_0)\frac{p_x^{\text{eq}}(0)}{k_BT}. \tag{1.9}$$

Now we can expand $p_x(0;\lambda)$ and keep up to the linear order in λ to get

$$p_x(0;\lambda) = p_x^{\text{eq}}(0) + \lambda(V_x - \langle V\rangle_0)\frac{p_x^{\text{eq}}(0)}{k_BT} + o(\lambda) \tag{1.10}$$

Therefore the average $\langle Q(t)\rangle_\lambda$ for $t > 0$ can be evaluated as

$$\langle Q(t)\rangle_\lambda = \sum_{xy} Q_x G_{xy}(t) p_y(0;\lambda) \tag{1.11}$$

Plugging in the expansion of $p_x(0;\lambda)$ in (1.10) we get

$$\langle Q(t)\rangle_\lambda = \langle Q(t)\rangle_0 + \lambda \sum_{xy} Q_x G_{xy}(t)(V_y - \langle V\rangle_0)\frac{p_y^{\text{eq}}(0)}{k_BT} + o(\lambda) \tag{1.12}$$

$$= \langle Q(t)\rangle_0 + \frac{\lambda}{k_BT}\text{Cov}^{\text{eq}}[Q(t), V(0)] + o(\lambda) \tag{1.13}$$

with $\text{Cov}^{\text{eq}}[Q(t), V(0)]$ the two time covariance function evaluated at equilibrium without perturbation. Comparing this expansion with (1.3), and using the time homogeneity (1.4) as well as our

perturbation scheme, we obtain

$$\int_{-\infty}^{0} R_{Q,V}(t-s)ds = \frac{1}{k_B T}\text{Cov}^{\text{eq}}[Q(t), V(0)]. \tag{1.14}$$

On the other hand we have

$$\int_{-\infty}^{0} R_{Q,V}(t-s)ds = \int_{t}^{+\infty} R_{Q,V}(s)ds. \tag{1.15}$$

Taking derivative with respect to t and noting the causality of $R_{Q,V}(t)$, we finally obtain the expression for the linear response function

$$R_{Q,V}(t) = -\frac{\Theta(t)}{k_B T}\frac{d}{dt}\text{Cov}^{\text{eq}}[Q(t), V(0)], \tag{1.16}$$

as is known as the equilibrium FDT.

This well-known relation turns out to have an important role in probing the physical properties of equilibrium thermodynamic systems because we can get the same information by measuring either the responses or the corresponding fluctuations and thus we have the flexibility when making choices. For example, in microrheology experiment [30], the response of a probe particle to an external force can be measured through its position correlation function, which is easily obtained through real-time imaging. In addition to the application in experiments as a technique, the FDT also provides important insights to the design of nanodevices. Since the fluctuations are related to noises and responses are related to sensitivity, the FDT suggests that at equilibrium a high sensitivity inevitably comes with a high noise. This means equilibrium is not good for a measurement device and a device has to be out of equilibrium in order to combine sensitivity with low noise.

Such insights motivate us to study the nonequilibrium statistical physics. And based on the early success of equilibrium FDT, different approaches have been attempted to study responses to perturbations using correlation functions.

1.4 Nonequilibrium Fluctuation Dissipation Relation (FDR)

In far-from-equilibrium, the responses can also generally be related to correlation functions and in this section we list several different versions of the nonequilibrium FDR.

Agarwal derived the nonequilibrium FDR in [15] for diffusive systems that can be described by the Fokker-Planck equation (FPE). It is shown that the nonequilibrium FDR has the same form of its equilibrium counterpart if we replace role of the energy U in section 1.3 by $-k_BT\ln\pi(x)$ with $\pi(x)$ being the NESS distribution. To be specific, the response function due to a perturbation in the external driving force is given by

$$R_{Q,x}(t) = -\frac{\Theta(t)}{k_BT}\frac{d}{dt}\text{Cov}[Q(t), x(0)], \tag{1.17}$$

which can also be written as [15]

$$R_{Q,x}(t) = -\text{Cov}[Q(t), \frac{\partial}{\partial x}\ln\pi(x)]. \tag{1.18}$$

Further, Prost, Joanny and Parrondo showed in [16] that for any system with Markovian dynamics if we choose the observable involved in the correlation function to be conjugated to the external force with respect to the "potential" corresponding to the NESS probability distribution, we can get the FDT that is identical to the equilibrium case. Since the NESS probability distribution is typically unknown, it is difficult to directly use the nonequilibrium FDT except for simple single particle systems [31].

Besides, Baiesi, Maes and Wynants showed in [32] that the nonequilibrium response can be written as

$$R_{Q,V}(t,s) = \frac{\Theta(t-s)}{2k_BT}\frac{d}{ds}\text{Cov}[Q(t), V(s)] - \frac{1}{2}\text{Cov}[\tau(\omega,s), Q(t)], \tag{1.19}$$

where the physical meaning of $\tau(\omega, s)$ is the first order excess activity.

Apparently the nonequilibrium FDT is generally different from the equilibrium FDT. However

it can also be shown that [33] the FDT for the NESS differs from that for the equilibrium state by an extra term involving the total entropy production. Many works have been done on the conditions where the equilibrium version of FDT is restored. It is shown that for a wide range of chemical reaction networks satisfying a certain sparseness condition and Poisson stationary distribution, an equilibrium-like FDT is restored [34]. Besides, it was pointed out that [35] for the "stalling current" in nonequilibrium system, the FDT takes the same form as that of the equilibrium case. This is experimentally verified for simple cases like one Brownian particle moving in a toroidal optical trap [36]. Some modified versions of the nonequilibrium FDT for the living systems like cells or bacteria are also experimentally validated [31].

1.5 Harada-Sasa Equality

The Harada-Sasa equality relates the violation of equilibrium FDT to the energy dissipation rate in a nonequilibrium steady state (NESS). A NESS is a state of a nonequilibrium system where the probability distribution does not change over time, which is what we study throughout this thesis. The Harada-Sasa equality was first derived for the Langevin system [20, 37] and then generalized to the field variables [38]. For a Langevin system with external force and small perturbation, the Harada-Sasa equality writes as:

$$\langle J\rangle_0 = \gamma\{v_s^2 + \int_{-\infty}^{+\infty}[\tilde{C}(\omega) - 2T\,\mathrm{Re}\,\tilde{R}(\omega)]\frac{d\omega}{2\pi}\}, \tag{1.20}$$

where $\langle J\rangle_0$ is the energy dissipation rate when perturbation $\lambda = 0$, v_s is the steady state velocity, and $\tilde{C}(\omega)$, $\tilde{R}(\omega)$ are Fourier transforms of the correlation and the response.

This equality has important applications in the study of biological molecule motors because it serves as a tool to estimate the energy dissipation rate from experimentally accessible quantities, irrespective of the details of the system [20]. It can also be used to experimentally examine the validity of the Langevin model [39].

1.6 Thermodynamic Bounds on Nonequilibrium Markov Jump Process

All the previous sections are about the equalities related to the response. In this section we introduce a different perspective where we use equalities and inequalities to study the nonequilibrium thermodynamics. The thermodynamic uncertainty relations (TUR) [22, 23, 24] provides bounds on the fluctuations by dissipation rates, which provides fundamental guiding principles in notechnological devices. Such perspective also motivates the recent study [27] on the generic responses for the finite state Markovian process. It is shown that the maginitude of generic static responses for such systems are bounded from above by quantities that depend on the type of the response and the thermodynamic force. Here we present the main results in detail.

A continuous-time Markov jump process on N states is described by the master equation

$$\dot{p}_i(t) = \sum_{j=1}^{N} W_{ij} p_j(t), \tag{1.21}$$

where W_{ij} are transition rates ($i \neq j$) and $W_{ii} = -\sum_{j \neq i} W_{ji}$. The steady-state probability distribution is given by $\sum_{j=1}^{N} W_{ij}\pi_j = 0$. The steady-state average of an observable is given by $\langle A \rangle_\pi = \sum_j A_j \pi_j$. In general we are able to make a decomposition

$$W_{ij} = \exp[-(B_{ij} - E_j - F_{ij}/2)], \tag{1.22}$$

with the vertex parameter E_j of each state, the symmetric edge parameter $B_{ij} = B_{ji}$ for each edge, and the asymmetric edge parameter $F_{ij} = -F_{ji}$ for each edge. A procedure based on the matrix tree theorem can be applied to express the stationary distribution in terms of those parameters and hence we can calculate the response of the stationary distribution. It turns out that universal constraints exist for those responses, irrespective of the structure of the underlying

transition dynamics. Those constraints are [27]

$$\frac{\partial \pi_i}{\partial E_j} = \pi_i \pi_j - \pi_i \delta_{ij}, \tag{1.23}$$

$$\left| \frac{\partial \pi_i}{\partial B_{mn}} \right| \leq \pi_i (1 - \pi_i) \tanh(F_{max}/4), \tag{1.24}$$

$$\left| \frac{\partial \pi_i}{\partial F_{mn}} \right| \leq \pi_i (1 - \pi_i). \tag{1.25}$$

The conditions where those bounds are saturated indicate the design principles for optimal response of devices. For example, for symmetric edge perturbation, maximal sensitivity is reached when there is a single cycle with strong timescale separation so that the system effectively has only two states [27] which suggests that small single-cycle systems are ideal for optimizing response.

The results obtained above for the discrete Markov jump processes also suggest many extensions, including the bounds on current responses, bounds on responses in diffusive systems and infinite state space chemical networks. More detailed information about the transition rates like the state-dependent temperature could also suggests interesting conclusions.

1.7 Fokker-Planck Equation

This whole thesis focuses on systems that can be modeled as diffusion processes. The Fokker-Planck Equation (FPE) [40], describes the time evolution of the probability density function for general diffusion processes. So in this section we give introduction to the FPE that we will use in chapter 2 and chapter 3. We can write the FPE using the Fokker-Planck operator $\hat{\mathcal{L}}$,

$$\partial_t p(\boldsymbol{x}, t) = \hat{\mathcal{L}} p(\boldsymbol{x}, t) \tag{1.26}$$

where

$$\hat{\mathcal{L}} = -\nabla \cdot [\boldsymbol{A}(\boldsymbol{x}, t) - \hat{\boldsymbol{B}}(\boldsymbol{x}, t) \nabla]. \tag{1.27}$$

Here $\boldsymbol{A}(\boldsymbol{x},t)$ is the drift vector and $\hat{\boldsymbol{B}}(\boldsymbol{x},t)$ is the diffusion matrix. The FPE can be written as a probability conservation equation

$$\partial_t p(\boldsymbol{x},t) = -\nabla \cdot \boldsymbol{J}(\boldsymbol{x},t) \tag{1.28}$$

with $\boldsymbol{J}$ the probability current

$$\boldsymbol{J}(\boldsymbol{x},t) = \boldsymbol{A}(\boldsymbol{x},t)p(\boldsymbol{x},t) - \hat{\boldsymbol{B}}(\boldsymbol{x},t)\nabla p(\boldsymbol{x},t). \tag{1.29}$$

It is noted that $\boldsymbol{J}$ is a signature of nonequilibrium system: the diffusion is at equilibrium if and only if $\boldsymbol{J} = 0$ everywhere.

The stochastic process satisfying the FPE (1.26) is equivalent to the Stratonovich stochastic differential equation

$$d\boldsymbol{x}(t) = \boldsymbol{A}(\boldsymbol{x},t)dt + \sqrt{2\hat{\boldsymbol{B}}(\boldsymbol{x},t)} \circ d\boldsymbol{W}(t), \tag{1.30}$$

where $\boldsymbol{W}(t)$ is a multidimensional Wiener process and $\circ$ denote the Stratonovich product. In the rest part of the thesis, we will constrain ourselves in time independent drift and diffusion parameters, i.e., $\boldsymbol{A}(\boldsymbol{x},t) = \boldsymbol{A}(\boldsymbol{x})$ and $\hat{\boldsymbol{B}}(\boldsymbol{x},t) = \hat{\boldsymbol{B}}(\boldsymbol{x})$.

In the following, we will introduce separately the diffusion process in 1D and 2D. There are many analytical results for the former, including the exact closed form solution for the steady state; while for the latter, we do not have such convenience. We will derived the results that are well known and will be used in the next several chapters here. The results are adapted from [40].

1.7.1 FPE in 1D

In 1D, the homogeneous FPE has the expression

$$\partial_t p(x,t) = -\partial_x[A(x)p(x,t)] + \partial_x[B(x)\partial_x p(x,t)]. \tag{1.31}$$

We are interested in the steady state solution $\pi(x)$ which satisfies

$$\frac{d}{dx}[A(x)\pi(x)] - \frac{d}{dx}[B(x)\partial_x\pi(x)] = 0, \tag{1.32}$$

which can also be written in terms of the probability current

$$\frac{d}{dx}J(x) = 0. \tag{1.33}$$

This has solution of a constant

$$J(x) = J. \tag{1.34}$$

If the process takes place on a non-periodic closed interval, the stationarity and continuity at the boundary points dictate $J = 0$, which means the system is in equilibrium. We will be focusing more on the nonequilibrium case, which suggests that we should be studying periodic boundary condition, which is a ring in 1D. Now we discuss the steady state solution on a ring of length L. There are two scenarios we want to present separately: equilibrium and nonequilibrium, which can be distinguished by whether the current is zero everywhere. First we study the equilibrium case. Setting $J = 0$, we have

$$A(x)\pi(x) = B(x)\frac{d}{dx}\pi(x), \tag{1.35}$$

for which the solution is

$$\pi(x) = \frac{\exp[\int_0^x A(x')/B(x')dx']}{\mathcal{N}}, \tag{1.36}$$

where $\mathcal{N}$ is the normalization constant or partition function

$$\mathcal{N} = \int_0^L \exp\left[\int_0^x \frac{A(x')}{B(x')}dx'\right]dx. \tag{1.37}$$

This solution is called potential solution. Note that if we consider the corresponding Langevin equation for Brownian particle moving in a energy landscape $U(x)$ with mobility $\mu(x)$ and $k_BT = 1$, then we would have $A(x) = -\mu(x)dU(x)/dx$, and $B(x) = \mu(x)$. Then the steady state distribution turns out to be a Boltzmann distribution, which we shall denote as π_{eq} since such solution only holds for equilibrium system

$$\pi_{\text{eq}}(x) = \frac{\exp[-U(x)]}{\mathcal{N}}. \tag{1.38}$$

Here we show that an application of the linear response theory for this equilibrium diffusive system would brings us the equilibrium static FDT. Consider an observable $Q(x)$ as a function of x, whose steady state average is

$$\langle Q \rangle_{\text{eq}} = \int_0^L Q(x)\pi_{\text{eq}}(x)dx. \tag{1.39}$$

Now consider a perturbation in the energy landscape

$$U(x) \to U_\lambda(x) = U(x) - \lambda V(x). \tag{1.40}$$

The corresponding stationary distribution density, which we shall call $\pi_{\text{eq}}(x;\lambda)$ to reflect the role of parameter λ, would be

$$\pi_{\text{eq}}(x;\lambda) = \frac{\exp[-U(x) + \lambda V(x)]}{\mathcal{N}(\lambda)}, \tag{1.41}$$

where $\mathcal{N}(\lambda)$ is the normalization constant with λ dependence. Therefore the response in $\pi_{\text{eq}}(x;\lambda)$ is

$$\partial_\lambda \pi_{\text{eq}}(x;\lambda)|_{\lambda=0} = \pi_{\text{eq}}(x)V(x) - \langle V \rangle_{\text{eq}}\pi_{\text{eq}}(x) \tag{1.42}$$

Therefore the response in the steady state average $\langle Q\rangle_{\text{eq}}$ is

$$\partial_\lambda \langle Q\rangle_{\text{eq}} = \int_0^L Q(x)\partial_\lambda \pi_{\text{eq}}(x)dx = \text{Cov}_{\text{eq}}(Q, V), \tag{1.43}$$

where $\text{Cov}_{\text{eq}}(Q, V)$ is the covariance of Q and V under the equilibrium distribtution π_{eq} and this is the static version of FDT.

So we emphasize on what we observed here: if the diffusive system has zero probability current everywhere, then system is at equilibrium and the steady state distribution is Boltzmann distribution. This result can be generalized to higher dimensions too, as is shown in chapter 5 in [40]. For such equilibrium system, we have FDT connecting the response and the correlation function.

Now if we have nonzero current

$$A(x)\pi(x) - B(x)\frac{d}{dx}\pi(x) = J \neq 0, \tag{1.44}$$

which happens when there is theormodynamic driving force, the system will be driven out of equilibrium. To solve it, it is convenient to define

$$\psi(x) = \exp[-\int_0^x A(x')/B(x')dx']. \tag{1.45}$$

Multiplying both side of (1.44) by $-\psi(x)/B(x)$ to get

$$\frac{d}{dx}[\pi(x)\psi(x)] = -J\frac{\psi(x)}{B(x)}. \tag{1.46}$$

It turns out that the current J in this expression is a fully determined constant. To show this, integrate the result on $[0, L]$ to get

$$\pi(x)\psi(x)|_0^L = -J\int_0^L \frac{\psi(x)}{B(x)}dx. \tag{1.47}$$

Because of the periodic boundary condition we know $\pi(0) = \pi(L)$ and thus we can solve for J,

$$J = \pi(0)\frac{1-\psi(L)}{\int_0^L \psi(x)/B(x)dx}. \tag{1.48}$$

Now we plug in the expression of J in (1.46) and integrate from 0 to x to get the desired density $\pi(x)$

$$\pi(x')\psi(x')|_0^x = -J\int_0^x \frac{\psi(x)}{B(x)}dx. \tag{1.49}$$

$$\pi(x) = \frac{\pi(0)}{\psi(x)}\frac{\int_x^L \psi(x')/B(x')dx' + \psi(L)\int_0^x \psi(x')/B(x')dx'}{\int_0^L \psi(x)/B(x)dx}. \tag{1.50}$$

Combing the constant factors together, we can also express it as

$$\pi(x) = \frac{1}{\mathcal{N}}\frac{\int_x^L \psi(x')/B(x')dx' + \psi(L)\int_0^x \psi(x')/B(x')dx'}{\psi(x)}. \tag{1.51}$$

So far we obtained the steady state solution of the general nonequilibrium FPE on a ring, which we will be using in the next chapter where we study the perturbation and response.

1.7.2 FPE in Higher Dimensions

Then we study the FPE in higher dimensions. For the most general FPE above 1D there is no closed form solution to the best of our knowledge. So we want to limit ourselves to some special cases so that we can still make some insightful predictions. To be specific we will be focusing on the form

$$\partial_t p(\boldsymbol{x}, t) = -\nabla \cdot \{\hat{\mu}(\boldsymbol{x})[-\nabla U(\boldsymbol{x}) + \boldsymbol{F}(\boldsymbol{x}) - \nabla]\}p(\boldsymbol{x}, t). \tag{1.52}$$

where $\hat{\mu}(\boldsymbol{x}) = \hat{\mu}$ is a constant, positive definite mobility matrix, $\boldsymbol{F}(\boldsymbol{x})$ is a nonconservative force field. Such diffusion system is at equilibrium if $\boldsymbol{F}(\boldsymbol{x}) = 0$, in which case the stationary distribution is again a Boltzmann distribution,

$$\pi(\boldsymbol{x}) = \frac{\exp[-U(\boldsymbol{x})]}{\mathcal{N}}, \tag{1.53}$$

which can be proven by directly solving the FPE in a same manner as the 1D case.

As we will show in later chapters, when $\nabla U(\boldsymbol{x}) = 0$ and $\boldsymbol{F}(\boldsymbol{x}) = \boldsymbol{f} \neq \mathbf{0}$, the steady state distribution is uniform due to the translational symmetry in the system. Now if we perturb the system parameters and observe the response of the steady state average of an observable, it turns out that there will be some interesting analytical predictions we can make. If $\nabla U(\boldsymbol{x}) \neq 0$ and $\boldsymbol{F}(\boldsymbol{x}) = \boldsymbol{f} \neq \mathbf{0}$, the steady state distribution is not uniform and we do not even have a closed form expression. It becomes hard to make any analytical prediction. We will study such system numerically.

CHAPTER 2

Thermodynamic Constraints on the Nonequilibrium Response of 1D Diffusion

This chapter is based on our work published in

[41] Qi Gao, Hyun-Myung Chun, and Jordan M. Horowitz. Thermodynamic constraints on the nonequilibrium response of one-dimensional diffusions. *Phys. Rev. E*, 105:L012102, Jan 2022.

2.1 Arbitrary Diffusion on a Ring

In this section we introduce our parametrization for the general diffusion model on a ring with length L. The dynamics of the diffusion, captured by (1.31), is determined by periodic functions $A(x)$ and $B(x)$. We can reparametrize them as

$$A(x) = \mu(x)(-U'(x) + f), \tag{2.1}$$

$$B(x) = \mu(x). \tag{2.2}$$

The notation in such parametrization is to resemble a mesoscopic Brownian particle moving in a viscous fluid with "mobility" $\mu(x)$ at temperature $k_BT = 1$. The "particle" has a potential "energy" $U(x)$ and is being driven by a constant driving "force" f. We will rely on this analogy for intuition, and often use this terminology. However, we stress that this is only a mathematical equivalence and our analysis is not restricted to a single overdamped particle, but applies to any

physical system that can be accurately modeled as a one-dimensional diffusion. Indeed, any model specified by $A(x)$ and $B(x)$ can be mapped to our parametrization. Moreover, our decomposition captures the most general separation of the dynamics into a conservative contribution $U(x)$ and a nonconservative contribution f. This highlights the fact that the only way to break the potential condition is the inclusion of a force with a constant contribution f, with the resulting thermodynamic force $\mathcal{F} = \int_0^L A(z)/B(z)dz = fL$. Thermodynamic equilibrium is then characterized by $f = \frac{1}{L}\int_0^L A(z)/B(z)dz = 0$, in which case the steady-state distribution takes the Gibbs form $\pi^{\rm eq}(x) \propto e^{-U(x)}$ in terms of the (dimensionless) energy landscape. For the nonequilibrium case where $f \neq 0$, the steady state distribution is derived in section 1.7

$$\pi(x) = \frac{1}{\mathcal{N}} \int_0^L dx' \mathcal{S}(x', x), \tag{2.3}$$

where

$$\mathcal{S}(x', x) = e^{U(x')-U(x)-f(x'-x)-\ln\mu(x')} \left[e^{-fL}\Theta(x - x') + \Theta(x' - x)\right], \tag{2.4}$$

$$\mathcal{N} = \int_0^L \int_0^L \mathcal{S}(x', x)\, dx'dx, \tag{2.5}$$

and $\Theta(z)$ is the Heaviside step function that is one for $z > 0$ and zero otherwise.

The main results of this chapter are listed as follows. Our first prediction is an equality for the response of an arbitrary observable Q to a coupled U and μ perturbation,

$$\frac{\delta\langle Q\rangle}{\delta U(y)} + \frac{\delta\langle Q\rangle}{\delta \ln\mu(y)} = -\pi(y)[Q(y) - \langle Q\rangle]. \tag{2.6}$$

For μ-perturbations, we derive an inequality on the ratio of the averages of two nonnegative observables Q_1 and Q_2 ($Q_1, Q_2 \geq 0$),

$$\left| \int_a^b \frac{\delta \ln(\langle Q_1\rangle/\langle Q_2\rangle)}{\delta \ln\mu(z)}\, dz \right| \leq \tanh(|\mathcal{F}|/4). \tag{2.7}$$

Note that the restriction to non-negative observables does not pose any serious limitation as we can always shift any observable by its minimum to create a non-negative one.

Last, we find that constraints on f perturbations can most naturally be expressed as responses to the thermodynamic force $\mathcal{F} = fL$,

$$\left| \frac{\partial \ln(\langle Q_1 \rangle / \langle Q_2 \rangle)}{\partial \mathcal{F}} \right| \leq 1. \tag{2.8}$$

By exploiting the freedom to choose the observables Q_1 and Q_2, we can arrive at bounds for a variety of quantities of interest. For example, the choice $Q_1(z; x) = \delta(z - x)$ and $Q_2 = 1$, gives bounds on the response of the steady-state density

$$\left| \int_a^b \frac{\delta \ln \pi(x)}{\delta \ln \mu(z)} \, dz \right| \leq \tanh(|\mathcal{F}|/4), \tag{2.9}$$

$$\left| \frac{\partial \ln \pi(x)}{\partial \mathcal{F}} \right| \leq 1. \tag{2.10}$$

We will prove these results in the following chapters.

2.2 Transformation of perturbations

In this section we show that any perturbation can be expressed by perturbations in μ, U and f, which can be analyzed individually and thus so will be the response formula. The FPE is fully determined by A and B, and thus any response comes from the perturbation in A and B too. We begin by deriving the mapping from A and B to μ, U and f. Then we use the mapping to decompose a general perturbation into perturbations of μ, U and f so that we can find the bound individually.

We first invert the parameterization in (2.1) and (2.2) to express μ, U and f in terms of A and B. By definition we have $\mu(x) = B(x)$. Next, we can eliminate μ by taking the ratios of (2.1) and

(2.2)

$$\frac{A(x)}{B(x)} = -U'(x) + f. \tag{2.11}$$

Exploiting the periodicity of U, we can integrate to single out

$$f = \frac{1}{L}\int_0^L \frac{A(z)}{B(z)}dz. \tag{2.12}$$

Substituting (2.12) back into (2.11) leads to a closed equation for U whose solution is,

$$U(x) = -\int_0^x \frac{A(z)}{B(z)}dz + \frac{x}{L}\int_0^L \frac{A(z)}{B(z)}dz + U(0), \tag{2.13}$$

with $U(0)$ an undetermined constant that has no affect on the dynamics.

With the transformation formulas, we are ready to study the transformation of perturbations. Imagine we apply a small perturbation by changing a control parameter by λ. Then the FPE is modified by a small amount as $A_\lambda(x) = A(x) + \lambda\delta A(x)$ and $B_\lambda(x) = B(x) + \lambda\delta B(x)$, where $\delta A(x)$ and $\delta B(x)$ are periodic functions conjugate to the perturbation λ. The response of the steady state to the perturbation in λ can then be expressed via the chain rule in terms of A and B functional derivatives as

$$\frac{\partial}{\partial\lambda} = \int_0^L dz\, \frac{\partial A_\lambda(z)}{\partial\lambda}\frac{\delta}{\delta A(z)} + \int_0^L dz\, \frac{\partial B_\lambda(z)}{\partial\lambda}\frac{\delta}{\delta B(z)} \tag{2.14}$$

$$= \int_0^L dz\, \delta A(z)\frac{\delta}{\delta A(z)} + \int_0^L dz\, \delta B(z)\frac{\delta}{\delta B(z)}. \tag{2.15}$$

Using the mapping in (2.2), (2.12), and (2.13), we can convert the functional derivatives with

respect to A and B via the chain rule as

$$\frac{\delta}{\delta A(z)} = \int_0^L ds\, \frac{\delta U(s)}{\delta A(z)} \frac{\delta}{\delta U(s)} + \int_0^L ds\, \frac{\delta \mu(s)}{\delta A(z)} \frac{\delta}{\delta \mu(s)} + \frac{\delta f}{\delta A(z)} \frac{\partial}{\partial f} \tag{2.16}$$

$$= \int_0^L ds \left(-\frac{\Theta(s-z)}{B(z)} + \frac{s}{L} \frac{1}{B(z)} \right) \frac{\delta}{\delta U(s)} + \frac{1}{L} \frac{1}{B(z)} \frac{\partial}{\partial f}, \tag{2.17}$$

and

$$\frac{\delta}{\delta B(z)} = \int_0^L ds\, \frac{\delta U(s)}{\delta B(z)} \frac{\delta}{\delta U(s)} + \int_0^L ds\, \frac{\delta \mu(s)}{\delta B(z)} \frac{\delta}{\delta \mu(s)} + \frac{\delta f}{\delta B(z)} \frac{\partial}{\partial f} \tag{2.18}$$

$$= \int_0^L ds \left(\Theta(s-z) \frac{A(z)}{B(z)^2} - \frac{s}{L} \frac{A(z)}{B(z)^2} \right) \frac{\delta}{\delta U(s)} + \frac{\delta}{\delta \mu(z)} - \frac{1}{L} \frac{A(z)}{B(z)^2} \frac{\partial}{\partial f}. \tag{2.19}$$

Substituting these expressions into the λ-derivative (2.15), we find after simplifying the integrals

$$\frac{\partial}{\partial \lambda} = \int_0^L ds\, \delta U(s) \frac{\delta}{\delta U(s)} + \int_0^L ds\, \delta \mu(s) \frac{\delta}{\delta \mu(s)} + \delta f \frac{\partial}{\partial f}, \tag{2.20}$$

where

$$\delta \mu(s) = \delta B(s) \tag{2.21}$$

$$\delta U(s) = -\int_0^s dz \, \left(\frac{\delta A(z) B(z) - A(z) \delta B(z)}{B(z)^2} \right) + \frac{s}{L} \int_0^L dz \, \left(\frac{\delta A(z) B(z) - A(z) \delta B(z)}{B(z)^2} \right) \tag{2.22}$$

$$\delta f = \frac{1}{L} \int_0^L dz \, \left(\frac{\delta A(z) B(z) - A(z) \delta B(z)}{B(z)^2} \right). \tag{2.23}$$

So far we transformed a general perturbation to perturbations of μ, U and f. To apply our constraints on the different types of response, we can express the general response as linear combinations of them

$$\frac{\partial}{\partial \lambda} = \int_0^L ds\, \delta U(s) \left(\frac{\delta}{\delta U(s)} + \frac{\delta}{\delta \ln \mu(s)} \right) + \int_0^L ds\, \big(\mu(s) \delta \mu(s) - \delta U(s) \big) \frac{\delta}{\delta \ln \mu(s)} + \delta f \frac{\partial}{\partial f} \tag{2.24}$$

2.3 Equilibrium-like FDT

In this section we elaborate and then prove (2.6).

2.3.1 Elaboration

In section 1.3 and 1.7 we showed that thermodynamic equilibrium ($\mathcal{F} = 0$), the response to perturbations in the energy landscape $U(x)$ is well characterized by the FDT in terms of equilibrium correlation functions. Away from thermodynamic equilibrium ($\mathcal{F} \neq 0$), the response to $U(x)$ perturbations is generally more challenging to characterize. However, when we combine changes in U with μ, the response turns out to be exactly equivalent to the response of an equilibrium Gibbs distribution to changes in U alone. We can exploit this observation by considering a perturbation that is equivalent to varying the energy and mobility in concert as $U_\lambda(x) = U(x) - \lambda V(x)$ and $\mu_\lambda(x) = \mu(x)[1 - \lambda V(x)]$. In this case, the response is

$$\partial_\lambda \langle Q \rangle = -\int_0^L V(z) \left[\frac{\delta \langle Q \rangle}{\delta U(z)} + \frac{\delta \langle Q \rangle}{\delta \ln \mu(z)} \right] dz. \tag{2.25}$$

Following our success with the equilibrium FDT, we want to express the response using correlations. Using (2.6), we can interpret the response as a simple FDT-like expression

$$\partial_\lambda \langle Q \rangle = \mathrm{Cov}(Q, V), \tag{2.26}$$

where significantly the response is given by the *nonequilibrium* covariance between the observable and the conjugate coordinate, $\mathrm{Cov}(Q, V) = \langle QV \rangle - \langle Q \rangle \langle V \rangle$. This result demonstrates that for a class of perturbations—where U and μ are varied in unison—the FDT holds in its equilibrium form, arbitrarily far from equilibrium. That an equilibrium-like FDT held for certain time-dependent perturbations of diffusion processes was previously observed by Graham [42].

2.3.2 Derivation

Now we prove (2.6). Let us proceed by first analyzing the derivatives on $\mathcal{S}(x', x)$ and $\mathcal{N}$ in expression (2.3):

$$\frac{\delta \mathcal{S}(x', x)}{\delta U(z)} + \frac{\delta \mathcal{S}(x', x)}{\delta \ln \mu(z)} = -\delta(x - z)\mathcal{S}(x', x), \qquad \frac{\delta \mathcal{N}}{\delta U(z)} + \frac{\delta \mathcal{N}}{\delta \ln \mu(z)} = -\mathcal{N}\pi(z). \tag{2.27}$$

Using these expressions, we then find for the derivative of $\pi(x)$,

$$\frac{\delta \pi(x)}{\delta U(z)} + \frac{\delta \pi(x)}{\delta \ln \mu(z)} = -\frac{1}{\mathcal{N}} \int_0^L dx' \delta(x - z)\mathcal{S}(x', x) - \frac{1}{\mathcal{N}^2} \left[-\mathcal{N}\pi(z)\right] \int_0^L dx' \mathcal{S}(x', x) \tag{2.28}$$

$$= -\pi(x)(\delta(x - z) - \pi(z)). \tag{2.29}$$

From this expression, we readily obtain equation (2.6) for the response of an observable $\langle Q \rangle = \int_0^L Q(x)\pi(x)dx$ as

$$\frac{\delta \langle Q \rangle}{\delta U(z)} + \frac{\delta \langle Q \rangle}{\delta \ln \mu(z)} = \int_0^L Q(x) \left[\frac{\delta \pi(x)}{\delta U(z)} + \frac{\delta \pi(x)}{\delta \ln \mu(z)} \right] dx = -\pi(z)(Q(z) - \langle Q \rangle). \tag{2.30}$$

2.4 Mobility Perturbation

In this section, we first prove the bound on the mobility perturbation response (2.7) and then show its applications.

2.4.1 Derivation

To evaluate the derivative in (2.7), we proceed by first differentiating $\mathcal{S}$ and $\mathcal{N}$,

$$\frac{\delta \mathcal{S}(x', x)}{\delta \ln \mu(z)} = -\delta(x' - z)\mathcal{S}(x', x), \qquad \frac{\delta \mathcal{N}}{\delta \ln \mu(z)} = -\int_0^L dy\, \mathcal{S}(z, y). \tag{2.31}$$

Consequently,

$$\frac{\delta\pi(x)}{\delta \ln \mu(z)} = -\frac{1}{\mathcal{N}}\mathcal{S}(z,x) + \frac{\pi(x)}{\mathcal{N}}\int_0^L dy\, \mathcal{S}(z,y). \tag{2.32}$$

With this expression, we can readily obtain an expression for the response of an observable as

$$\frac{\delta\langle Q\rangle}{\delta \ln \mu(z)} = \int_0^L Q(x)\left[-\frac{1}{\mathcal{N}}\mathcal{S}(z,x) + \frac{\pi(x)}{\mathcal{N}}\int_0^L dy\, \mathcal{S}(z,y)\right]dx \tag{2.33}$$

$$= -\frac{1}{\mathcal{N}}\int_0^L Q(x)\mathcal{S}(z,x)dx + \frac{\langle Q\rangle}{\mathcal{N}}\int_0^L \mathcal{S}(z,y)dy. \tag{2.34}$$

We are now in a position to evaluate the derivative in (2.7):

$$\int_a^b \frac{\delta \ln(\langle Q_1\rangle/\langle Q_2\rangle)}{\delta \ln \mu(z)}dz = \int_a^b \frac{\frac{\delta\langle Q_1\rangle}{\delta \ln \mu(z)}\langle Q_2\rangle - \frac{\delta\langle Q_2\rangle}{\delta \ln \mu(z)}\langle Q_1\rangle}{\langle Q_1\rangle\langle Q_2\rangle}dz. \tag{2.35}$$

Upon substitution of (2.34), we see that the terms linear in average of the observable in (2.34) cancel, leaving

$$\int_a^b \frac{\delta \ln(\langle Q_1\rangle/\langle Q_2\rangle)}{\delta \ln \mu(z)}dz = -\frac{1}{\mathcal{N}}\frac{\left(\int_a^b\int_0^L Q_1(x)S(z,x)dzdx\right)\langle Q_2\rangle - \left(\int_a^b\int_0^L Q_2(x)S(z,x)dzdx\right)\langle Q_1\rangle}{\langle Q_1\rangle\langle Q_2\rangle} \tag{2.36}$$

To simplify this expression, we note that average of any observable can also be expressed in terms of $\mathcal{S}$ as

$$\langle Q\rangle = \frac{1}{\mathcal{N}}\int_0^L\int_0^L Q(x)S(x',x)dx'dx. \tag{2.37}$$

Upon substitution of this formula into (2.36), we find that the result can be conveniently expressed in terms of the integrals

$$q_1 = \int_{z\in[a,b]} \int_0^L Q_1(x)\mathcal{S}(z,x)\, dxdz \tag{2.38}$$

$$\bar{q}_1 = \int_{z\notin[a,b]} \int_0^L Q_1(x)\mathcal{S}(z,x)\, dxdz \tag{2.39}$$

$$q_2 = \int_{z\in[a,b]} \int_0^L Q_2(x)\mathcal{S}(z,x)\, dxdz \tag{2.40}$$

$$\bar{q}_2 = \int_{z\notin[a,b]} \int_0^L Q_2(x)\mathcal{S}(z,x)\, dxdz \tag{2.41}$$

as

$$\int_a^b \frac{\delta \ln(\langle Q_1\rangle/\langle Q_2\rangle)}{\delta \ln \mu(z)} dz = \frac{q_1\bar{q}_2 - \bar{q}_2 q_1}{(\bar{q}_1+q_1)(\bar{q}_2+q_2)}. \tag{2.42}$$

The notation here is reminiscent of the derivation Ref. [43], which will allow us to import those methods directly.

Noting that $\bar{q}_1$, q_1, $\bar{q}_2$, and q_2 are all non-negative, the denominator of (2.42) is bounded by the inequality of arithmetic and geometric means:

$$(\bar{q}_1+q_1)(\bar{q}_2+q_2) = \bar{q}_1\bar{q}_2 + \bar{q}_1 q_2 + q_1\bar{q}_2 + q_1 q_2 \geq q_1\bar{q}_2 + \bar{q}_1 q_2 + 2\sqrt{\bar{q}_1\bar{q}_2 q_1 q_2} = (\sqrt{\bar{q}_1 q_2} + \sqrt{q_1\bar{q}_2})^2, \tag{2.43}$$

where the equality is saturated when $\bar{q}_1\bar{q}_2 = q_1 q_2$. The numerator can also be factored

$$q_2\bar{q}_1 - q_1\bar{q}_2 = (\sqrt{\bar{q}_1 q_2} - \sqrt{q_1\bar{q}_2})(\sqrt{\bar{q}_1 q_2} + \sqrt{q_1\bar{q}_2}). \tag{2.44}$$

The result is

$$\left| \int_a^b \frac{\delta \ln(\langle Q_1\rangle/\langle Q_2\rangle)}{\delta \ln \mu(z)} dz \right| \leq \left| \frac{\sqrt{\bar{q}_1 q_2} - \sqrt{q_1\bar{q}_2}}{\sqrt{\bar{q}_1 q_2} + \sqrt{q_1\bar{q}_2}} \right| = \tanh\left(\frac{1}{4} \left| \ln \frac{q_1\bar{q}_2}{\bar{q}_1 q_2} \right| \right). \tag{2.45}$$

Our last step is to bound the ratio $q_1\bar{q}_2/\bar{q}_1 q_2$:

$$\frac{q_1\bar{q}_2}{\bar{q}_1 q_2} = \frac{\int_0^L \int_0^L dx_1 dx_0 \int_{z_1\in[a,b]} dz_1 \int_{z_0\notin[a,b]} dz_0\, Q_1(x_0)Q_2(x_1)\mathcal{S}(z_1,x_0)\mathcal{S}(z_0,x_1)}{\int_0^L \int_0^L dx_1 dx_0 \int_{z_1\in[a,b]} dz_1 \int_{z_0\notin[a,b]} dz_0\, Q_1(x_0)Q_2(x_1)\mathcal{S}(z_0,x_0)\mathcal{S}(z_1,x_1)} \tag{2.46}$$

$$= \frac{\int_0^L \int_0^L dx_1 dx_0 \int_{z_1\in[a,b]} dz_1 \int_{z_0\notin[a,b]} dz_0\, W(x_0,x_1,z_0,z_1)\frac{\mathcal{S}(z_1,x_0)\mathcal{S}(z_0,x_1)}{\mathcal{S}(z_0,x_0)\mathcal{S}(z_1,x_1)}}{\int_0^L \int_0^L dx_1 dx_0 \int_{z_1\in[a,b]} dz_1 \int_{z_0\notin[a,b]} dz_0\, W(x_0,x_1,z_0,z_1)}, \tag{2.47}$$

where we introduced the four-dimensional non-negative weight function

$$W(x_0,x_1,z_0,z_1) = Q_1(x_0)Q_2(x_1)\mathcal{S}(z_0,x_0)\mathcal{S}(z_1,x_1) \geq 0. \tag{2.48}$$

Therefore the ratio $q_1\bar{q}_2/\bar{q}_1 q_2$ can be viewed as the weighted average of an observable ($\langle\cdot\rangle_W$), which we can bound by its maximum as

$$\frac{q_1\bar{q}_2}{\bar{q}_1 q_2} = \left\langle \frac{\mathcal{S}(z_1,x_0)\mathcal{S}(z_0,x_1)}{\mathcal{S}(z_0,x_0)\mathcal{S}(z_1,x_1)} \right\rangle_W \tag{2.49}$$

$$\leq \max_{\{z_0,z_1,x_0,x_1\}} \frac{\mathcal{S}(z_1,x_0)\mathcal{S}(z_0,x_1)}{\mathcal{S}(z_0,x_0)\mathcal{S}(z_1,x_1)} \tag{2.50}$$

$$= \max_{\{z_0,z_1,x_0,x_1\}} \frac{\left[e^{-fL}\Theta(x_0-z_1)+\Theta(z_1-x_0)\right]\left[e^{-fL}\Theta(x_1-z_0)+\Theta(z_0-x_1)\right]}{\left[e^{-fL}\Theta(x_0-z_0)+\Theta(z_0-x_0)\right]\left[e^{-fL}\Theta(x_1-z_1)+\Theta(z_1-x_1))\right]} \tag{2.51}$$

$$= e^{|f|L}, \tag{2.52}$$

where the last equality holds when, for example, $f > 0$ and $z_0 > x_1 > z_1 > x_0$. Equation (2.7) follows immediately.

2.4.2 Application: Energy Perturbation Response

As we have seen in section 1.3 and 1.7, changes in the energy function U represent a customary perturbation applied to probe a system's steady state. While it can be challenging to interpret expressions for the response in this case, we can combine the predictions in (2.6) and (2.7) on the mobility perturbation response to find simple thermodynamic constraints for energy perturbation response. To combine (2.6) and (2.7), we have to focus on a perturbation where we shift the energy

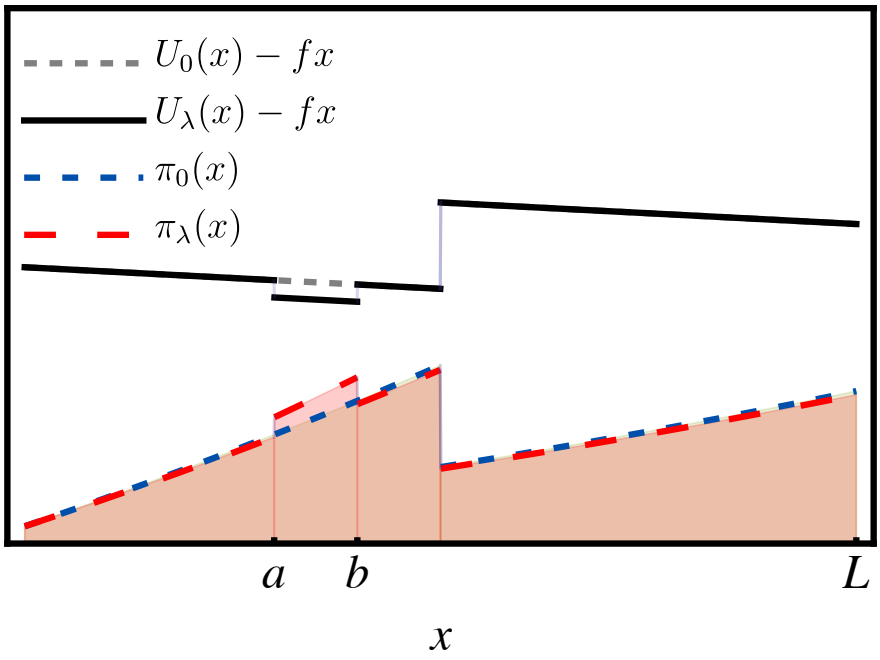

Figure 2.1: Example of perturbing the energy landscape: Pictured is the "effective potential" as a function of position x before the perturbation $U_0(x) - fx$ (gray dashed) and after lowering the energy in the region $x \in [a, b]$ by $\lambda I_{[a,b]}(x)$ (black). This shifts the steady state distribution $\pi(x)$ from the orange dotted curve to the red long-dashed curve.

uniformly on a fixed interval $x \in [a, b]$ (Fig. 2.1): specifically, $U_\lambda(x) = U(x) - \lambda I_{[a,b]}(x)$, where $I_A(z)$ is the indicator function taking the value 1 when z is in the set A and 0 otherwise. Our question is then how thermodynamics constrains the nonequilibrium response

$$R^{\text{neq}}_{Q,U} = \partial_\lambda \langle Q \rangle = -\int_a^b \frac{\delta \langle Q \rangle}{\delta U(z)} dz \tag{2.53}$$

of a (nonnegative) observable Q to perturbations in U with fixed thermodynamic driving $\mathcal{F}$. Before addressing this question, however, let us first remind ourselves what a naive application of the FDT (1.43) would have predicted, namely that the response would be given by the covariance between the observable $Q(x)$ and the conjugate coordinate $I_{[a,b]}(x)$ as

$$R^{\text{eq}}_{Q,U} = \text{Cov}\left(Q, I_{[a,b]}\right). \tag{2.54}$$

Now, let us proceed with perturbations of a nonequilibrium steady state ($\mathcal{F} \neq 0$). Observe that U perturbations can be built from the sum

$$\begin{aligned} R^{\mathrm{neq}}_{Q,U} &= -\int_a^b \frac{\delta\langle Q\rangle}{\delta U(z)} dz \\ &= -\int_a^b \left[\frac{\delta\langle Q\rangle}{\delta U(z)} + \frac{\delta\langle Q\rangle}{\delta \ln \mu(z)}\right] - \frac{\delta\langle Q\rangle}{\delta \ln \mu(z)} dz. \end{aligned} \tag{2.55}$$

The first term is our coupled μ-U perturbation (2.25) that satisfies an equilibrium-like FDT (2.26) and is therefore equal to the covariance between the observable Q and the conjugate coordinate $I_{[a,b]}$, $\mathrm{Cov}\left(Q, I_{[a,b]}\right)$, which is exactly the same as our naive prediction for the equilibrium response $R^{\mathrm{eq}}_{Q,U}$. The remaining contribution can be constrained by the thermodynamic force using (2.7) with the choices $Q_1(x) = Q(x)$ and $Q_2(x) = 1$,

$$\begin{aligned} \left|R^{\mathrm{neq}}_{Q,U} - R^{\mathrm{eq}}_{Q,U}\right| &= \left|\langle Q\rangle \int_a^b \frac{\delta \ln\langle Q\rangle}{\delta \ln \mu(z)} dz\right| \\ &\leq \langle Q\rangle \tanh(|\mathcal{F}|/4). \end{aligned} \tag{2.56}$$

The farther the system is from equilibrium, as measured by the force $\mathcal{F}$, the larger the possible nonequilibrium response. Alternatively, since $R^{\mathrm{eq}}_{Q,U}$ is the naive prediction from the FDT, we can interpret (2.56) as a quantitative bound on the violation of the FDT in terms of the nonequilibrium driving.

To illustrate this prediction on energy perturbation, we analyzed the response of the steady-state density $\pi(x)$ itself, corresponding to the observable $Q(z;x) = \delta(z-x)$. Denoting this response with a slight abuse of notation as $R^{\mathrm{neq}}_{x,U}$, the operative form of (2.56) is

$$\left|R^{\mathrm{neq}}_{x,U} - R^{\mathrm{eq}}_{x,U}\right| \leq \pi(x) \tanh(|\mathcal{F}|/4) \tag{2.57}$$

We choose perturbations of the energy landscape of the form $U(x) = U_0\Theta(x - L/2)$ where $\Theta(x - L/2)$ is the Heaviside step function and $U_0 \in \{1, 2, 3\}$ is a constant (Fig. 2.1). We further fix the mobility $\mu(x) = 1$ and set the circumference of the circle to $L = 1$. We numerically evaluated

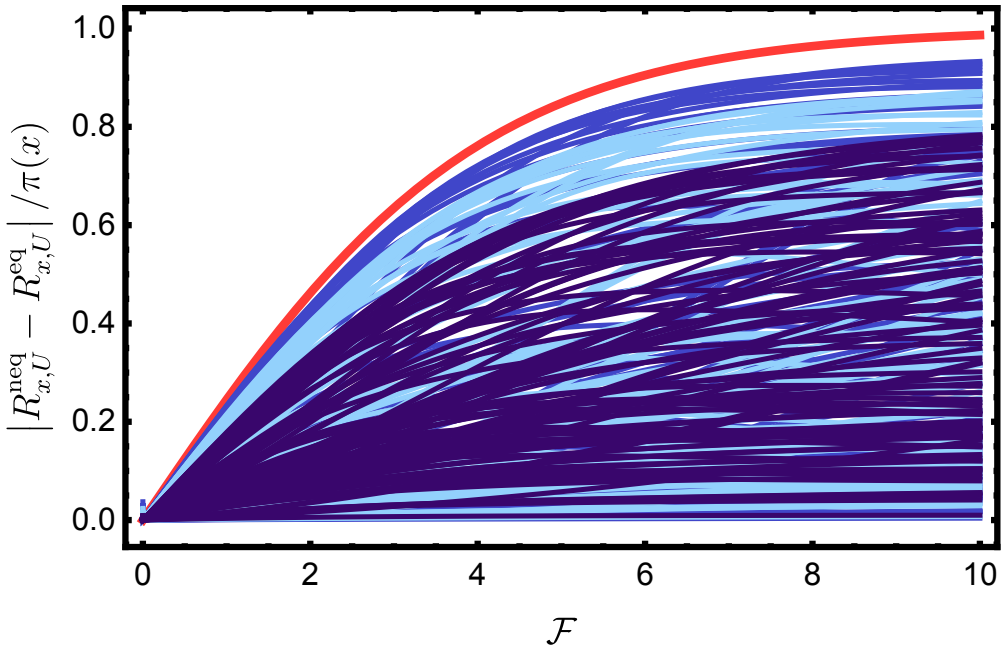

Figure 2.2: Illustration of energy-perturbation thermodynamic bound: Normalized deviation of nonequilibrium response $\left|R^{\rm neq}_{x,U} - R^{\rm eq}_{x,U}\right|/\pi(x)$ at position x for energy perturbations on the interval $[a, b]$ from an energy landscape $U(x) = U_0\Theta(x - L/2)$ given by the Heaviside step function multiplied by $U_0 = 1$ (dark blue), 2 (light blue), 3 (blue). Each color contains 100 randomly sampled pairs $(x = a)$ on the unit square. All curves fall below the predicted bound $\tanh(|\mathcal{F}|/4)$ (red line). Other parameters: $L = 1$ and $\mu(x) = 1$.

the response $R^{\rm neq}_{x,U}$ to energy perturbations on the interval $[x, b]$ as a function of $\mathcal{F} = f$ for 100 combinations of x and b each sampled uniformly on the unit interval $[0, 1]$. We have chosen the observation position x to be on the edge of the perturbation region in order to enhance the sampling of highly responsive scenarios.

The results presented in Fig. 2.2 verify that for all sampled parameter combinations the normalized deviation $\left|R^{\rm neq}_{x,U} - R^{\rm eq}_{x,U}\right|/\pi(x)$ remains below the predicted bound $\tanh(|\mathcal{F}|/4)$.

2.5 Force Perturbation

In this section we prove (2.8). For the convenience of the actual proof, we express it in a slightly modified form

$$\left|\frac{\partial \ln(\langle Q_1\rangle/\langle Q_2\rangle)}{\partial f}\right| \leq L. \tag{2.58}$$

To organize the derivatives with respect to the force f, we will find it convenient to use the function

$$\mathcal{O}(x',x) = (x'-x+L)\Theta(x-x') + (x'-x)\Theta(x'-x), \tag{2.59}$$

which we note for later use is bounded $0 \leq \mathcal{O} \leq L$. Then, we have

$$\frac{\partial \mathcal{S}(x',x)}{\partial f} = -\mathcal{O}(x',x)\mathcal{S}(x',x), \qquad \frac{\partial \mathcal{N}}{\partial f} = -\int_0^L \int_0^L dx'dx\ \mathcal{O}(x',x)\mathcal{S}(x',x), \tag{2.60}$$

so that

$$\frac{\partial \pi(x)}{\partial f} = -\frac{1}{\mathcal{N}}\int_0^L dx' \mathcal{O}(x',x)\mathcal{S}(x',x) + \frac{\pi(x)}{\mathcal{N}}\int_0^L \int_0^L dx'dx''\ \mathcal{O}(x',x'')\mathcal{S}(x',x''). \tag{2.61}$$

As a result the response of an observable can be expressed as

$$\frac{\partial \langle Q\rangle}{\partial f} = -\frac{1}{\mathcal{N}}\int_0^L \int_0^L dx'dx\ Q(x)\mathcal{O}(x',x)\mathcal{S}(x',x) + \frac{\langle Q\rangle}{\mathcal{N}}\int_0^L \int_0^L dx'dx\ \mathcal{O}(x',x)\mathcal{S}(x',x). \tag{2.62}$$

With these formulas in hand, we can now address the derivative in (2.58). Upon substitution of (2.62) into the left hand side of (2.58), we find that the second terms in (2.62) linear in the average of the observables cancel, resulting in the expression

$$\left|\frac{\partial \ln(\langle Q_1\rangle/\langle Q_2\rangle)}{\partial f}\right| = \left|\frac{\int_0^L \int_0^L dx'dx\ \mathcal{O}(x',x)Q_2(x)\mathcal{S}(x',x)}{\int_0^L \int_0^L dx'dx\ Q_2(x)\mathcal{S}(x',x)} - \frac{\int_0^L \int_0^L dx'dx\ \mathcal{O}(x',x)Q_1(x)\mathcal{S}(x',x)}{\int_0^L \int_0^L dx'dx\ Q_1(x)\mathcal{S}(x',x)}\right|, \tag{2.63}$$

after simplification using the definition of $\mathcal{N}$. A particularly useful interpretation presents itself after we note that $Q(x)\mathcal{S}(x',x) \geq 0$. Therefore each ratio can be interpreted as a normalized average of $\mathcal{O}$ with observable-dependent weight $Q(x)\mathcal{S}(x',x) \geq 0$, which we denote as $\langle\cdot\rangle_Q$. The result is that we can express (2.63) as

$$\left|\frac{\partial \ln(\langle Q_1\rangle/\langle Q_2\rangle)}{\partial f}\right| = \left|\langle\mathcal{O}\rangle_{Q_2} - \langle\mathcal{O}\rangle_{Q_1}\right| \leq L, \tag{2.64}$$

where the bound follows from $0 \leq \mathcal{O} \leq L$, completing the derivation.

2.6 Connection to Markov Jump Processes

The aim of this section is to discuss the relationship between the present study and previous work on thermodynamic limitations to steady-state response in discrete Markov jump processes [43].

2.6.1 Review of thermodynamic limits to response for discrete Markov jump processes

As we are only interested in stochastic processes on a ring, we will introduce the ideas and results from Ref. [43] specialized to this context.

We have in mind a system of N discrete states at positions $x_i = i\Delta x$ around a ring of length $L = N\Delta x$. We label these states as of $i = 0, \ldots, N$, where we identify the redundant state $i = N$ with $i = 0$ to enforce the periodic boundary conditions. The probability to find the system in state i at time t is then governed by the Master equation [40]

$$\dot{p}_i(t) = \sum_{j=0}^{N-1} W_{ij} p_j(t), \tag{2.65}$$

where the off-diagonal entries of the transition rate matrix W_{ij} specify the probability per unit time to jump from state j to state i, and $W_{ii} = -\sum_{j\neq i} W_{ji}$. As only nearest-neighbor hops are allowed,

the only nonzero transition rates are those for which i and j differ by one; thus, all rates are of the form $W_{i+1,i}$ or $W_{i-1,i}$, corresponding to 'right' and 'left' hops. As the state space is irreducible, a unique stationary distribution π_i exists and can be obtained as the solution of

$$\sum_{j=0}^{N-1} W_{ij}\pi_j = 0. \tag{2.66}$$

Thermodynamics is included in the model by identifying the log-ratio of rates around cycles as the thermodynamic force driving the system out of equilibrium. As a ring only has a single cycle, the sole thermodynamic force is

$$F_C = \ln \frac{W_{0,N-1}\cdots W_{2,1}W_{1,0}}{W_{N-1,0}\cdots W_{1,2}W_{0,1}}. \tag{2.67}$$

Reference [43] introduced a parameterization of the transition rate matrix in terms of vertex parameters E_i, symmetric edge parameters $B_{i+1,i} = B_{i,i+1}$, and asymmetric edge parameters $F_{i+1,i} = -F_{i,i+1}$:

$$W_{i+1,i} = e^{-(B_{i+1,i}-E_i-F_{i+1,i}/2)}, \qquad W_{i-1,i} = e^{-(B_{i,i-1}-E_i+F_{i,i-1}/2)}. \tag{2.68}$$

Nonequilibrium effects are included in this parameterization solely through the asymmetric edge parameters, which can be seen by substituting this decomposition into the definition of the thermodynamic force (2.67) to conclude

$$F_C = \sum_{i=0}^{N-1} F_{i+1,i}. \tag{2.69}$$

The main predictions of Ref. [43] are then a series of equalities and inequalities for the derivative of the steady state distribution with respect to these three parameter families. Here, we present forms most relevant for our present discussion.

Vertex parameters: An equality for vertex parameter perturbations can be obtained from

Eq. (13) of Ref. [43],

$$\sum_{j=0}^{N-1} V_j \frac{\partial \langle Q \rangle}{\partial E_j} = -\sum_{j=0}^{N-1} V_j \pi_j (Q_j - \langle Q \rangle) = -\mathrm{Cov}(Q, V), \tag{2.70}$$

where the state space observable V_i is the conjugate coordinate to the perturbation.

Symmetric edge parameters: If we perturb the $B_{i+1,i}$ of all the edges between a pair of nodes at positions $x_a = a\Delta x$ and $x_b = b\Delta x$ then Eq. (20) of Ref. [43] predicts

$$\left| \sum_{i=a}^{b-1} \frac{\partial \ln(\langle Q_1 \rangle / \langle Q_2 \rangle)}{\partial B_{i+1,i}} \right| \leq \tanh(|F_C|/4). \tag{2.71}$$

Asymmetric edge parameters: For perturbations of all the $F_{i+1,i}$ all the way around the ring, one can deduce from Eq. (21) of Ref. [43] using techniques in that paper an equality of the form,

$$\left| \sum_{i=0}^{N-1} \frac{\partial \ln(\langle Q_1 \rangle / \langle Q_2 \rangle)}{\partial F_{i+1,i}} \right| \leq N, \tag{2.72}$$

although this expression does not explicitly appear.

It is the continuous limits of these formulas that are operative for diffusion processes. To make this connection, we first have to develop the mapping between this discrete Markov jump process and its limit as a continuous diffusion process, obtained as the spacing between lattice points tends to zero, $\Delta x \to 0$.

2.6.2 Discrete approximation of a continuous diffusion process

Motivated by the structure of the decomposition of the transition rate matrix in (2.68), we now look to construct a Markov jump process that has a well defined continuous limit as a diffusion process, and that maintains that structure.

To begin, we first introduce a smooth probability density $\rho(x, t)$ such that the probability the system is between $x_i - \Delta x/2$ and $x_i + \Delta x/2$ at time t is given by $\rho(x_i, t) = p_i(t)/\Delta x$. We also

introduce three more smooth functions of space $E(x)$, $B(x)$ and f such that

$$E(x_i) = E_i \tag{2.73}$$

$$B(x_i) = B_{i+1,i} = B_{i,i+1} \tag{2.74}$$

$$f\Delta x = F_{i+1,i} = -F_{i,i+1}. \tag{2.75}$$

Notice that we have assigned the "location" of $B_{i+1,i}$ to the position with the smaller index. In addition, to have a well-defined limit the asymmetric edge parameters need to be linear in Δx, and a constant value is sufficient to include all possible nonconservative effects. In terms of these functions, the transition rates (2.68) become

$$W_+(x_i) \equiv W_{i+1,i} = e^{-(B(x_i)-E(x_i)-f\Delta x/2)} \tag{2.76}$$

$$W_-(x_i) \equiv W_{i-1,i} = e^{-(B(x_{i-1})-E(x_i)+f\Delta x/2)} = e^{-(B(x_i-\Delta x)-E(x_i)+f\Delta x/2)}, \tag{2.77}$$

and thermodynamic force (2.67) simplifies to $F_C = \sum_{i=0}^{N-1} f\Delta x = fL$.

With this setup the procedure to carry out the limit $\Delta x \to 0$ is as follows: We substitute these definitions into the Master equation (2.65), expand for small Δx, and then diffusively rescale time $t \to t/\Delta x^2$. The result is the Fokker-Planck equation

$$\partial_t \rho(x,t) = -\partial_x \left[e^{-(B(x)-E(x))}(E'(x) - f)\rho(x,t)\right] + \partial_x \left[e^{-(B(x)-E(x))}\partial_x \rho(x,t)\right]. \tag{2.78}$$

This is of the form of the FPE. Codifying the observation that interesting results in the discrete case corresponding to separate perturbations in the E, B, and f functions, suggests the identification

$$\mu(x) = \exp\big(E(x) - B(x)\big), \quad U(x) = E(x). \tag{2.79}$$

2.6.3 Diffusion limits of thermodynamic bounds

Having established a consistent discretization of our diffusion process, we turn to utilizing the thermodynamic bounds for discrete Markov processes (2.70) - (2.72) to prove the analogous thermodynamic bounds for the continuous limit.

In making this connection, we will repeatedly face the situation where we have to convert a derivative with respect to a finite collection of variables, like the $\{E_i\}$ or $\{B_{i+1,i}\}$, into a functional derivative as the spacing tends to zero ($\Delta x \to 0$). In preparation for these calculations, we first present this relationship in general and then exploit it in the following. To this end, let us consider two smooth functions $f(x)$ and $g(x)$, and the functional $\mathcal{I}[f]$. In the discrete picture, we only evaluate these functions at the positions x_i, with values $f(x_i)$ and $g(x_i)$. The functional is then a function $\mathcal{I}(\{f(x_i)\})$ of the finite set of values $\{f(x_i)\}$, but is assumed to tend smoothly to $\mathcal{I}(\{f(x_i)\}) \to \mathcal{I}[f]$ as $\Delta x \to 0$. With this setup, as $\Delta x \to 0$ the definitions of the derivative and functional derivative are connected by

$$\lim_{\Delta x \to 0} \sum_{i=0}^{N-1} g(x_i) \frac{\partial \mathcal{I}(\{f(x_i)\})}{\partial f(x_i)} = \int_0^L g(x) \frac{\delta \mathcal{I}[f]}{\delta f(x)} dx. \tag{2.80}$$

Let us now address each type of perturbation in turn.

Vertex parameters: For the vertex derivatives, we first replace $E_i = E(x_i)$ and $V_i = V(x_i)$, and then take the continuous limit

$$\lim_{\Delta x \to 0} \sum_{j=0}^{N-1} V_j \frac{\partial \langle Q \rangle}{\partial E_j} = \lim_{\Delta x \to 0} \sum_{j=0}^{N-1} V(x_j) \frac{\partial \langle Q \rangle}{\partial E(x_j)} = \int_0^L V(x) \frac{\delta \langle Q \rangle}{\delta E(x)} dx, \tag{2.81}$$

where we used (2.80) with $\mathcal{I} = \langle Q \rangle$, $f(x) = E(x)$, and $g(x) = V(x)$. Inserting this expression into (2.70) and applying the identification $U(x) = E(x)$ (2.79), we arrive at expression equivalent to Eq. (2.26).

Symmetric edge parameters: When we perturb all the symmetric edge parameters between

positions $x_a = a\Delta x$ and $x_b = b\Delta x$, we obtain the response in the continuous limit by first replacing $B_{i+1,i} = B(x_i)$, and then

$$\lim_{\Delta x\to 0}\sum_{i=a}^{b-1}\frac{\partial \ln(\langle Q_1\rangle/\langle Q_2\rangle)}{\partial B_{i+1,i}} = \lim_{\Delta x\to 0}\sum_{i=a}^{b-1}\frac{\partial \ln(\langle Q_1\rangle/\langle Q_2\rangle)}{\partial B(x_i)} = \int_{x_a}^{x_b}\frac{\delta \ln(\langle Q_1\rangle/\langle Q_2\rangle)}{\delta B(x)}dx, \quad (2.82)$$

where we have utilized (2.80), with $\mathcal{I} = \ln(\langle Q_1\rangle/\langle Q_2\rangle)$, $f(x) = B(x)$, and $g(x) = I_{[a,b]}(x)$ is the indicator function on the set $x \in [a, b]$. Substituting into (2.71), noting the change of variables $\delta \ln \mu(x) = -\delta B(x)$ (with $E(x)$ fixed) from (2.79), and that the sole thermodynamic force is $F_C = fL$ we arrive at Eq. (2.7).

Asymmetric edge parameters: Lastly, for asymmetric edge perturbations, we link the f-perturbations via

$$\left|\frac{\partial \ln(\langle Q_1\rangle/\langle Q_2\rangle)}{\partial f}\right| = \left|\lim_{\Delta x\to 0}\sum_{i=1}^{N}\frac{\partial \ln(\langle Q_1\rangle/\langle Q_2\rangle)}{\partial(F_{i+1,i}/\Delta x)}\right| \leq \lim_{\Delta x\to 0} N\Delta x = L, \quad (2.83)$$

where the inequality is due to (2.72), and the desired result Eq. (2.8) follows.

2.6.4 Failure of bounds in the continuous limit for higher dimensions

It turns out that the results known for discrete Markov process [43] are not sufficient to constrain the steady-state response of diffusion processes in higher dimensions.

To demonstrate this possibility, we focus here on a two-dimensional diffusion process with positions (x, y) on a torus whose circumferences in both directions are L. As before, we discretize the dynamics by placing the evolution on a square lattice with lattice spacing l, and discretized positions $(x_i, y_j) = (il, jl)$. The transition rates are only nonzero for nearest neighbor hops in the positive and negative x and y directions. Motivated by our previous discussion we introduce the smooth functions defined on the torus, $B_x(x, y)$, $B_y(x, y)$, $E(x, y)$, f_x and f_y, allowing us to

specify the transition rates

$$W^{j}_{i+1,i} = e^{-(B_x(x_i,y_j)-E(x_i,y_j)-f_x l/2))} \tag{2.84}$$

$$W^{j}_{i-1,i} = e^{-(B_x(x_{i-1},y_j)-E(x_i,y_j)+f_x l/2)} \tag{2.85}$$

$$W^{j+1,j}_{i} = e^{-(B_y(x_i,y_j)-E(x_i,y_j)-f_y l/2)} \tag{2.86}$$

$$W^{j-1,j}_{i} = e^{-(B_y(x_i,y_{j-1})-E(x_i,y_j)+f_y l/2)}. \tag{2.87}$$

For similar reasons as above, these rates limit to a diffusion process as $l \to 0$

Now imagine we perturb all the symmetric edge parameters in a square region from $x_a = al$ to $x_b = bl$ and from $y_{a'} = a'l$ to $y_{b'} = b'l$, totaling $N_{\rm e} = (b-a)(b'-a'-1) + (b-a-1)(b'-a')$ edges. Now Eq. (20) of Ref. [43] predicts that the response is no worse than the number of *vertices on the perimeter* of this region $N_{\rm p} = 2(b-a+b'-a')$ as

$$\left| \sum_{i=a}^{b-1} \sum_{j=a'}^{b'-1} \left(\frac{\partial \ln(\langle Q_1 \rangle / \langle Q_2 \rangle)}{\partial B_x(x_i,y_j)} + \frac{\partial \ln(\langle Q_1 \rangle / \langle Q_2 \rangle)}{\partial B_y(x_i,y_j)} \right) \right| \leq N_{\rm p} - 1. \tag{2.88}$$

In the continuous limit $l \to 0$, the left hand side tends to a finite value given by the functional derivative

$$\lim_{l\to 0} \sum_{i=a}^{b-1} \sum_{j=a'}^{b'-1} \left(\frac{\partial \ln(\langle Q_1 \rangle / \langle Q_2 \rangle)}{\partial B_x(x_i,y_j)} + \frac{\partial \ln(\langle Q_1 \rangle / \langle Q_2 \rangle)}{\partial B_y(x_i,y_j)} \right) = \int_{x_a}^{x_b} \int_{y_{a'}}^{y_{b'}} \frac{\delta \ln(\langle Q_1 \rangle / \langle Q_2 \rangle)}{\delta B_x(x,y)} + \frac{\delta \ln(\langle Q_1 \rangle / \langle Q_2 \rangle)}{\delta B_y(x,y)} dy dx. \tag{2.89}$$

However, the right hand side tends to infinity, since the number of vertices on the perimeter grows without bound as the spacing tends to zero. Thus, the inequalities derived in Ref. [43] for discrete Markov processes are uninformative in the continuous limit in dimensions above one.

CHAPTER 3

Response on Mobility Perturbations in Higher Dimensional Diffusions

This chapter is based on a manuscript we are currently working on:

Qi Gao, Hyun-Myung Chun, and Jordan M. Horowitz. Thermodynamic constraints on kinetic perturbation response in nonequilibrium two-dimensional homogeneous diffusions (in preparation).

3.1 Setup

In this section we present the setup for the system. We study the stationary response of the FPE on a N-dimensional torus $\Omega = [0,1] \times [0,1] \times [0,1] \ldots \times [0,1]$. The system's configuration $\boldsymbol{x}(t) = (x_1(t), \ldots x_N(t))$ at time t takes values in Ω and the FPE describing the time-evolution of the probability density $p(\boldsymbol{x}, t)$ for this class of systems can be parameterized as

$$\partial_t p(\boldsymbol{x}, t) = -\nabla \cdot \{\hat{\mu}(\boldsymbol{x})[-\nabla U(\boldsymbol{x}) + \boldsymbol{F}(\boldsymbol{x}) - \nabla]\} p(\boldsymbol{x}, t) \tag{3.1}$$

$$\equiv \mathcal{L} p(\boldsymbol{x}, t). \tag{3.2}$$

Similar to what we did in chapter 2, here we borrow language from the modeling of a colloidal particle in a viscous fluid to identify a position-dependent mobility matrix $\hat{\mu}(\boldsymbol{x})$ and split the force into a conservative part due to potential $U(\boldsymbol{x})$ and a nonconservative part $\boldsymbol{F}(\boldsymbol{x})$ ($\nabla \times \boldsymbol{F}(\boldsymbol{x}) \neq 0$).

We assume the system relaxes to a unique steady-state distribution $\pi(\boldsymbol{x})$ given as the solution of the stationary FPE

$$\mathcal{L}\pi(\boldsymbol{x}) = 0. \tag{3.3}$$

In general, this steady state solution is not known in the sense that we do not know its closed form solution. As we mentioned in section 1.7, when the "potential condition" is statisfied [40], which means for our parameterization $\boldsymbol{F}(\boldsymbol{x}) = 0$, then the steady-state distribution is a Gibbs distribution which we identify as an equilibrium distribution.

Without a full analytic solution to the FPE in dimensions higher than one, to make progress we proceed with a simpler classes of model where $\hat{\mu}(\boldsymbol{x}) = \hat{\mu}$ is a constant mobility matrix and the nonconservative driving $\boldsymbol{F}(\boldsymbol{x}) = \boldsymbol{f} = (f_1, \ldots, f_N)$ is uniform. In our main results, we need to further assume $U(\boldsymbol{x}) = 0$ and mobility matrix $\hat{\mu} = \text{diag}(\mu, \mu)$ is diagonal and uniform. The simplification under such settings is two-fold. First, with $\boldsymbol{F}(\boldsymbol{x}) = \boldsymbol{f}$, the steady state distribution has translational symmetry and thus should be uniform. Since the size of region Ω, $|\Omega| = 1$, we know $\pi(\boldsymbol{x}) = 1$. Second, the Fokker-Planck operator $\hat{\mathcal{L}}$ in Fourier basis is diagonal, and thus the Fourier coefficient of the response $\delta\pi(\boldsymbol{x})$ are separated from each other, making it straightforward to evaluate the response. We will show this in detail in later sections. We consider the mobility perturbation scheme

$$\hat{\mu} \to \hat{\mu}[1 + \lambda S(\boldsymbol{x})] \tag{3.4}$$

and study the response in the average of observable Q

$$R_{SQ} = \partial_\lambda \langle Q \rangle = \int_\Omega S(\boldsymbol{z}) \frac{\delta \langle Q \rangle}{\delta \ln \mu(\boldsymbol{z})} d\boldsymbol{z}. \tag{3.5}$$

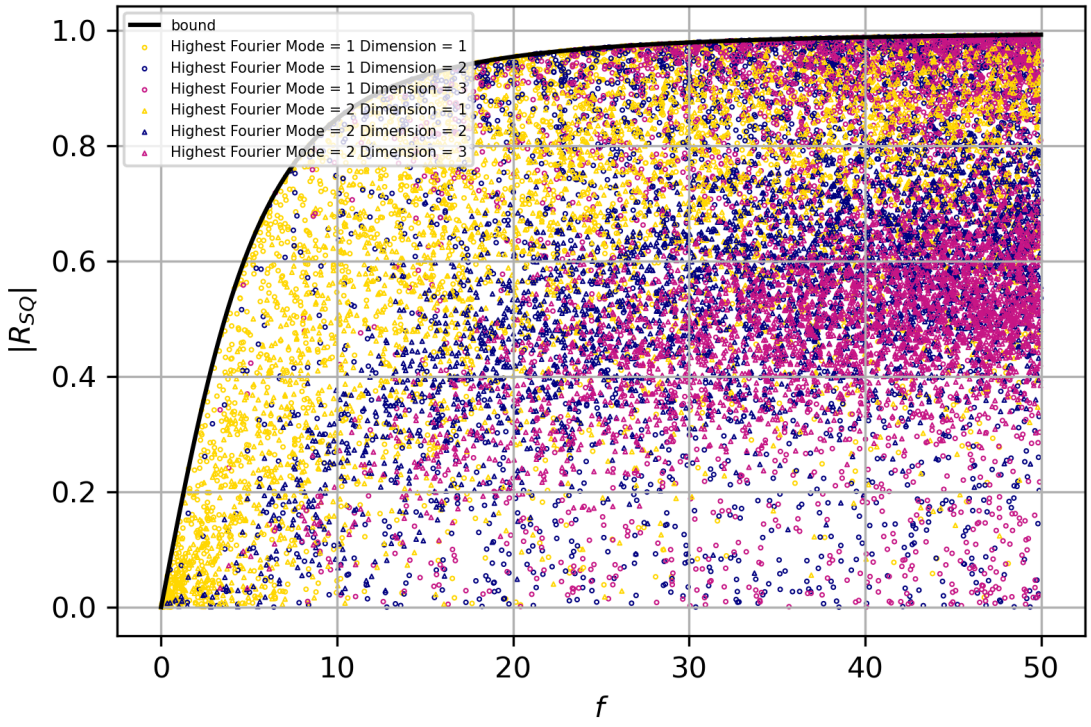

Figure 3.1: Illustration of the bound for general mobility perturbation response $|R_{SQ}|$: Random sampling of f, S and Q while fixing $\mathrm{Var}(S) = \mathrm{Var}(Q) = 1$. Each color contains 3000 data points. We set $a_{\boldsymbol{m}} = 0$ and $b_{\boldsymbol{m}} = 0$ for certain $\boldsymbol{m}$ for an enhanced visual effect.

3.2 Main Results

In this section we present the main results with illustrations.

3.2.1 General Mobility Perturbation

The first main result is the bound

$$|\partial_\lambda \langle Q \rangle| \leq \sqrt{\frac{\mathrm{Var}(S)\mathrm{Var}(Q)}{1 + (2\pi/\mathcal{F})^2}}, \tag{3.6}$$

where $\mathcal{F} = \max_j |f_j|$ quantifies how far the system is out of equilibrium. As a sanity check, when $\mathcal{F} = 0$, the system is at equilibrium, and the bound is zero, meaning there is no violation of FDT.

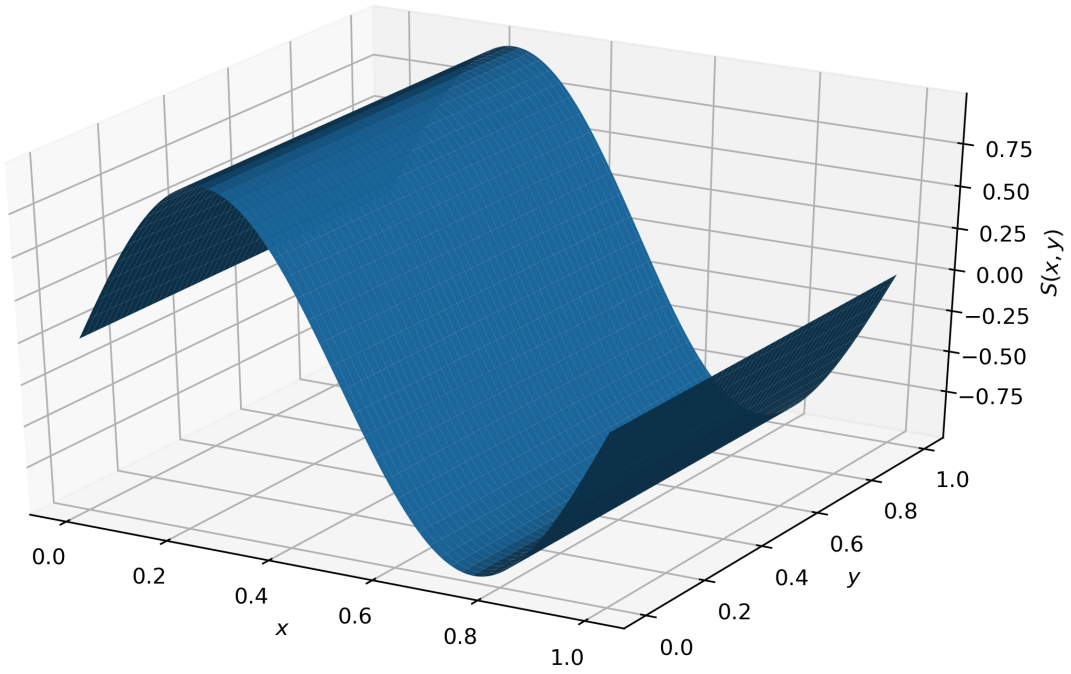

Figure 3.2: Example of S that saturates the bound for general mobility perturbation response $|R_{SQ}|$ (3.6) in 2D, when $\boldsymbol{f} = (f_x, f_y)$ and $|f_x| > |f_y|$: $S(\boldsymbol{x}) = S(x, y) = \sin(2\pi x)$.

Fig. 3.1 provides numerical evidence for this bound. In this plot, we fix $\mathrm{Var}(S) = \mathrm{Var}(Q) = 1$ and randomly sample their Fourier coefficients with some cutoff on the highest Fourier mode M (because the computer can only deal with finite number of modes). As we can see in the plot, the lower the cutoff and the dimension, the easier it is for the maximal response to reach the bound, because the optimal response is reached when the highest Fourier mode is 1 and it is more likely to reach saturation when M is small.

The saturation of the bound (3.6) for non-constant S and Q is that, S and Q are sinusoidal with period 1 or uniform in the directions corresponding to $\mathcal{F}$ and uniform in other orthogonal directions. In 2D, for $\boldsymbol{f} = (f_x, f_y)$ and $|f_x| > |f_y|$, an example of such S is $S(\boldsymbol{x}) = S(x, y) = \sin(2\pi x)$, as is shown in Fig. 3.2.

3.2.2 Special Case

In our second main result, we specialize even further to a situation where S and Q are the same and given by an indicator function $S(\boldsymbol{x}) = Q(\boldsymbol{x}) = \delta_{\mathcal{S}}(\boldsymbol{x})$, taking the value one on the region of the state space $\mathcal{S} \subseteq \Omega$ of size $|\mathcal{S}|$, and zero otherwise. In this case, the expected value of our Q is simply the probability to be in $\mathcal{S}$, $\langle \delta_{\mathcal{S}} \rangle = \pi(\mathcal{S}) = |\mathcal{S}|$. In this case the response satisfies the tighter inequality

$$|R_{\mathcal{S}}| = |\partial_\lambda \langle \delta_{\mathcal{S}} \rangle| \leq \frac{\pi(\mathcal{S})(1 - \pi(\mathcal{S}))}{1 + (2\pi/\mathcal{F})^2} = \frac{\mathrm{Var}(\delta_{\mathcal{S}})}{1 + (2\pi/\mathcal{F})^2}. \tag{3.7}$$

The improvement comes from the denominator being $1 + (2\pi/\mathcal{F})^2 \geq \sqrt{1 + (2\pi/\mathcal{F})^2}$. This inequality (3.7) is numerically verified in Fig. 3.3. Since the computer can only deal with finite numbers, we approximate the arbitrary shape $\mathcal{S}$ by dividing Ω uniformly into several small blocks. Then we randomly choose from those blocks to approximate the random sampling of perturbation region $\mathcal{S}$. As we can see, all points fall below the predicted limit (3.7) (the red line). It is noted though, this bound is not saturated. We notice that, all sampled points appear to fall below the same limit independent of the dimension of the system. This suggests that the limit can be determined from the maximum response in one dimension, which can be calculated from the one-dimensional analytic solution of the response (2.34) by choosing $\mathcal{S} = [0, 1/2]$,

$$|R_{\mathcal{S}}| = |\partial_\lambda \langle \delta_{\mathcal{S}} \rangle| \leq \frac{1}{4} - \frac{1}{\mathcal{F}} \tanh(\frac{\mathcal{F}}{4}). \tag{3.8}$$

This limit (3.8), which we shall denote as $|R_{\text{ring}}|$, is pictured by the black line in Fig. 3.3. While we have observed this bound numerically, we have not been able to prove it analytically. We notice that in one-dimension, the responses form several lines. This is because the number of blocks in this case is small so there are just a small number of possible independent combinations when selecting the perturbation blocks.

Numerics shows that the saturation condition for 2D is $\mathcal{S}$ occupies exact half of region and

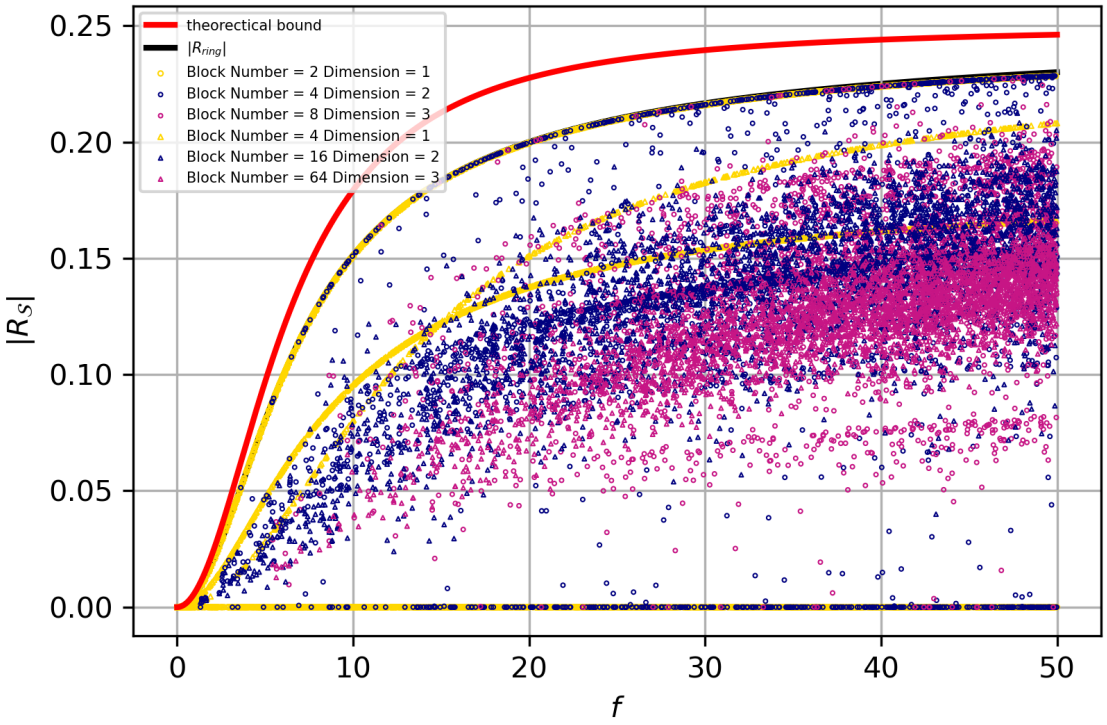

Figure 3.3: Illustration of the bound for special mobility perturbation response $|R_{\mathcal{S}}|$: Random sampling of $\boldsymbol{f}$, $\mathcal{S}$. Each color contains 3000 data points. We divide the unit square into several blocks and randomly select from them to form the perturbation region. The smaller the block number is, the more probable it is to form an optimal perturbation region to saturate the numerical bound.

takes a "belt shape" which goes around the torus in the direction of the smaller absolute force. For example, in 2D if we have $\boldsymbol{f} = (f_x, f_y)$ with $|f_x| > |f_y|$, then the optimal $\mathcal{S}$ that saturates the bound (3.8) is $\mathcal{S} = [0, \frac{1}{2}] \times [0, 1]$ (as is shown in Fig. 3.4), together with all the equivalent regions due to translational symmetry.

Our analytical results shown in this section can be proved using Fourier expansion and optimization. In section 3.3, we want to first introduce the Fourier expansion approach to solve for the distribution and mobility response in more general FPE where $U(\boldsymbol{x}) \neq 0$. From that we can see why it is necessary to proceed with the extra assumption of a flat potential. Then in section 3.4 we introduce the optimization technique based on Lagrangian multiplier method.

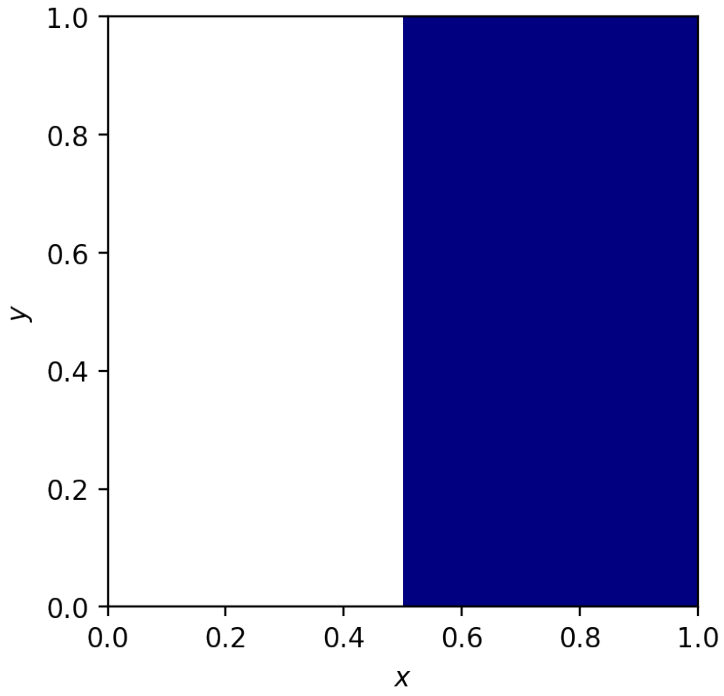

Figure 3.4: Example of the optimal region for special mobility perturbation response $|R_{\mathcal{S}}|$ that saturate the bound (3.8) in 2D when $|f_x| > |f_y|$: $\mathcal{S} = [0, \frac{1}{2}] \times [0, 1]$. Here $\mathcal{S}$ is the white region where the mobility is perturbed uniformly and the navy blue region is unperturbed.

3.3 The Fourier Expansion Approach

In this section we introduce the Fourier expansion approach used for solving the response. When introducing this approach, we can reduce our restrictions on the potential and mobility. To be specific we consider arbitrary $U(\boldsymbol{x})$ and arbitrary uniform mobility matrix $\hat{\mu}$. We denote the Fourier basis as

$$e_{\boldsymbol{m}}(\boldsymbol{r}) = e^{i2\pi \boldsymbol{m}\cdot\boldsymbol{r}} \tag{3.9}$$

for $\boldsymbol{m} = (m_1, \ldots, m_N) \in \mathbb{Z}^N$. The Fourier expansion for an general periodic function $G(\boldsymbol{r})$ on Ω is

$$G(\boldsymbol{r}) = \sum_{\boldsymbol{m}} G_{\boldsymbol{m}} e_{\boldsymbol{m}}(\boldsymbol{r}), \tag{3.10}$$

where the Fourier coefficient $G_{\boldsymbol{m}}$ is given by

$$G_{\boldsymbol{m}} = \int_{\Omega} G(\boldsymbol{r}) e^*_{\boldsymbol{m}}(\boldsymbol{r}) d\boldsymbol{r}, \tag{3.11}$$

with $e^*_{\boldsymbol{m}}(\boldsymbol{r})$ the complex conjugate of $e_{\boldsymbol{m}}(\boldsymbol{r})$. We will be using this set of Fourier expansion notations for $U(\boldsymbol{x})$ and $\pi(\boldsymbol{x})$.

We have two goals in mind when introducing the Fourier transform here. The first is to find the NESS distribution $\pi(\boldsymbol{x})$. The second goal is to evaluate the mobility perturbation response $\delta\pi(\boldsymbol{x})$. As we will see, we can express $\pi(\boldsymbol{x})$ and $\delta\pi(\boldsymbol{x})$ as a series but there are few analytical statements we can make about them due to the complexity the potential $U(\boldsymbol{x})$ brings.

Now we start calculating $\pi(\boldsymbol{x})$ by plugging the Fourier expansion of each term into the stationary FPE (3.3), which gives

$$\sum_{\boldsymbol{m}} (\mathcal{L}\pi)_{\boldsymbol{m}} e^{i2\pi \boldsymbol{m}\cdot\boldsymbol{x}} = 0, \tag{3.12}$$

with

$$(\mathcal{L}\pi)_{\boldsymbol{m}} = -\sum_{\boldsymbol{m}'} \Big[(4\pi^2 \boldsymbol{m}\cdot\hat{\mu}\boldsymbol{m} + i2\pi \boldsymbol{m}\cdot\hat{\mu}\boldsymbol{f})\delta_{\boldsymbol{m}',\boldsymbol{m}} + 4\pi^2 U_{\boldsymbol{m}-\boldsymbol{m}'} \boldsymbol{m}\cdot\hat{\mu}(\boldsymbol{m}-\boldsymbol{m}') \Big] \pi_{\boldsymbol{m}'}. \tag{3.13}$$

From this we are able to define the Fourier component of $\mathcal{L}$ as a matrix

$$\mathcal{L}_{\boldsymbol{m},\boldsymbol{m}'} = -(4\pi^2 \boldsymbol{m}\cdot\hat{\mu}\boldsymbol{m} + i2\pi \boldsymbol{m}\cdot\hat{\mu}\boldsymbol{f})\delta_{\boldsymbol{m}',\boldsymbol{m}} - 4\pi^2 U_{\boldsymbol{m}-\boldsymbol{m}'} \boldsymbol{m}\cdot\hat{\mu}(\boldsymbol{m}-\boldsymbol{m}'). \tag{3.14}$$

Here we abuse the notation $\mathcal{L}$ to denote the Fokker-Planck operator and its matrix representation in Fourier basis interchangeably. A difficulty here is that, $\mathcal{L}_{\mathbf{0},\boldsymbol{m}'} = 0, \forall \boldsymbol{m}'$, meaning $\mathcal{L}$ is not exactly invertible. As we will see next, we can get around this difficulty by introducing a modified Fokker-Planck operator (matrix) $\tilde{\mathcal{L}}$ and consider a decomposition of it. The insight behind the modification of $\tilde{\mathcal{L}}$ is to incorporate the normalization condition

$$\pi_{\mathbf{0}} = \int_{\Omega} \pi(\boldsymbol{r}) d\boldsymbol{r} = 1, \tag{3.15}$$

to replace the redundancy produced by $\mathcal{L}_{\mathbf{0},\boldsymbol{m}'} = 0, \forall \boldsymbol{m}'$ in $\mathcal{L}\pi = 0$. Before we apply this normalization condition, we introduce the decomposition. We can decompose $\mathcal{L}$ in (3.14) into the diagonal "flat" part and the off-diagonal "U" part,

$$\mathcal{L}_{\boldsymbol{m},\boldsymbol{m}'} = \mathcal{L}^0_{\boldsymbol{m},\boldsymbol{m}'} - \mathcal{L}^U_{\boldsymbol{m},\boldsymbol{m}'}, \tag{3.16}$$

where

$$\mathcal{L}^0_{\boldsymbol{m},\boldsymbol{m}'} = -(4\pi^2 \boldsymbol{m} \cdot \hat{\mu} \boldsymbol{m} + i 2\pi \boldsymbol{m} \cdot \hat{\mu} \boldsymbol{f}) \delta_{\boldsymbol{m}',\boldsymbol{m}} \tag{3.17}$$

is the the flat-potential Fokker-Planck operator and

$$\mathcal{L}^U_{\boldsymbol{m},\boldsymbol{m}'} = 4\pi^2 U_{\boldsymbol{m}-\boldsymbol{m}'} \boldsymbol{m} \cdot \hat{\mu} (\boldsymbol{m} - \boldsymbol{m}'). \tag{3.18}$$

Now we are ready to modify $\mathcal{L}$ to make it invertible. We define the modified Fokker-Planck matrix by adding 1 to the element right in the middle of $\mathcal{L}$, i.e. $\mathcal{L}_{\mathbf{0},\mathbf{0}}$,

$$\tilde{\mathcal{L}}_{\boldsymbol{m},\boldsymbol{m}'} := \mathcal{L}_{\boldsymbol{m},\boldsymbol{m}'} + \delta_{\boldsymbol{m},\mathbf{0}} \delta_{\boldsymbol{m}',\mathbf{0}}. \tag{3.19}$$

To see how this would help to evaluate the inverse, we note that if we require the modification of

$\mathcal{L}$ is done by defining the modified "diagonal part",

$$\tilde{\mathcal{L}}^0_{\boldsymbol{m},\boldsymbol{m}'} := \mathcal{L}^0_{\boldsymbol{m},\boldsymbol{m}'} + \delta_{\boldsymbol{m},\boldsymbol{0}}\delta_{\boldsymbol{m}',\boldsymbol{0}}, \tag{3.20}$$

which is invertible and then $\tilde{\mathcal{L}}$ can be decomposed as

$$\tilde{\mathcal{L}}_{\boldsymbol{m},\boldsymbol{m}'} = \tilde{\mathcal{L}}^0_{\boldsymbol{m},\boldsymbol{m}'} - \mathcal{L}^U_{\boldsymbol{m},\boldsymbol{m}'}, \tag{3.21}$$

which allows us to write down the inverse as a series,

$$\begin{aligned}
\tilde{\mathcal{L}}^{-1} &= (\tilde{\mathcal{L}}^0 - \mathcal{L}^U)^{-1} && (3.22)\\
&= \left[\tilde{\mathcal{L}}^0[I - \frac{\mathcal{L}^U}{\tilde{\mathcal{L}}^0}]\right]^{-1} && (3.23)\\
&= [I - \frac{\mathcal{L}^U}{\tilde{\mathcal{L}}^0}]^{-1}(\tilde{\mathcal{L}}^0)^{-1} && (3.24)\\
&= \sum_{j=0}^{\infty}(\frac{\mathcal{L}^U}{\tilde{\mathcal{L}}^0})^j(\tilde{\mathcal{L}}^0)^{-1} && (3.25)
\end{aligned}$$

where by convention,

$$\frac{\mathcal{L}^U}{\tilde{\mathcal{L}}^0} = (\tilde{\mathcal{L}}^0)^{-1}\mathcal{L}^U. \tag{3.26}$$

Now we can evaluate π from the modified Fourier FPE

$$\sum_{\boldsymbol{m}'} \tilde{\mathcal{L}}_{\boldsymbol{m},\boldsymbol{m}'}\pi_{\boldsymbol{m}'} = \delta_{\boldsymbol{m},\boldsymbol{0}} \tag{3.27}$$

by inverting $\tilde{\mathcal{L}}$

$$\pi_{\boldsymbol{m}} = \sum_{\boldsymbol{m}'} \tilde{\mathcal{L}}^{-1}_{\boldsymbol{m},\boldsymbol{m}'}\delta_{\boldsymbol{m}',\boldsymbol{0}} \tag{3.28}$$

So far we achieved the first major goal of evaluating the π, and the next step is to solve the

response in the Fourier linear response equations,

$$(\mathcal{L}\delta\pi)_{\boldsymbol{m}} = -(\delta\mathcal{L}\pi)_{\boldsymbol{m}}. \tag{3.29}$$

We consider the mobility perturbation scheme

$$\hat{\mu} \to \hat{\mu}[1 + \lambda S(\boldsymbol{x})] \tag{3.30}$$

and study the response in the average of observable Q

$$\partial_\lambda \langle Q \rangle = \int_\Omega S(\boldsymbol{z}) \sum_{i,j=1}^{N} \frac{\delta\langle Q\rangle}{\delta \ln \mu_{ij}(\boldsymbol{z})} d\boldsymbol{z} \tag{3.31}$$

Again the derivative is take only on $\pi(\boldsymbol{x})$ so we need to evaluate $\delta\pi$. Once we have $\delta\pi$ the desired response follows as

$$\partial_\lambda \langle Q \rangle = \sum_{\boldsymbol{m}} \delta\pi_{\boldsymbol{m}} Q_{-\boldsymbol{m}}. \tag{3.32}$$

Now we want to evaluate $(\delta\mathcal{L}\pi)_{\boldsymbol{m}}$ so that we can use (3.29) to evaluate $\delta\pi_{\boldsymbol{m}}$. We explicitly allow the Fokker-Planck operator to depend on the external parameter via

$$\mathcal{L}_\lambda = -\nabla \cdot \hat{\mu}[1 + \lambda S(\boldsymbol{x})][-\nabla U(\boldsymbol{x}) + \boldsymbol{f}] + \nabla \cdot \hat{\mu}\nabla \tag{3.33}$$

$$\equiv \mathcal{L} + \lambda\delta\mathcal{L} \tag{3.34}$$

Then we can write down the Fourier expansion of $\delta\mathcal{L}\pi$,

$$(\delta\mathcal{L}\pi)_{\boldsymbol{m}} = -\int_\Omega \{[\nabla \cdot \hat{\mu} S(\boldsymbol{x})][-\nabla U(\boldsymbol{x}) + \boldsymbol{f}]\pi(\boldsymbol{x})\} e^*_{\boldsymbol{m}}(\boldsymbol{x}) d\boldsymbol{x}. \tag{3.35}$$

To make progress from here becomes very challenging. Although we can in principle write down the full Fourier expansion and study the responses by numerically sampling a variety of

potentials, there is no definite conclusions we can make about the responses. This is why we narrow down on a class of special cases where there is no potential $U(\boldsymbol{x}) = 0$.

3.4 Derivation

In this section we derive the analytical results using the Fourier expansion method. Under the assumption $U(\boldsymbol{x}) = 0$ and $\hat{\mu} = \text{diag}(\mu, \mu)$, $e_{\boldsymbol{m}}$ is the eigenfunction of the Fokker-Planck operator $\mathcal{L}$ with eigenvalue $l_{\boldsymbol{m}} = -(4\pi^2 \boldsymbol{m}\hat{\mu} \cdot \boldsymbol{m} + i2\pi \boldsymbol{m} \cdot \hat{\mu}\boldsymbol{f})$. In this case we begin by evaluating $\delta\pi_{\boldsymbol{m}}$,

$$\delta\pi_{\boldsymbol{m}} = -(\delta\hat{\mathcal{L}}\pi)_{\boldsymbol{m}}/l_{\boldsymbol{m}}, \boldsymbol{m} \neq \boldsymbol{0}, \tag{3.36}$$

$$\delta\pi_{\boldsymbol{0}} = 0. \tag{3.37}$$

All we need is to evaluate $(\delta\hat{\mathcal{L}}\pi)_{\boldsymbol{m}}$,

$$(\delta\hat{\mathcal{L}}\pi)_{\boldsymbol{m}} = -\int_{\Omega} [\nabla S(\boldsymbol{r}) \cdot \hat{\mu}\boldsymbol{f}] e^*_{\boldsymbol{m}}(\boldsymbol{r}) d\boldsymbol{r}, \tag{3.38}$$

$$= -i2\pi S_{\boldsymbol{m}} \boldsymbol{m} \cdot \hat{\mu}\boldsymbol{f}, \tag{3.39}$$

where $S_{\boldsymbol{m}}$ is the Fourier coefficient of $S(\boldsymbol{x})$ and in the last step we used integration by parts. Combining this with (3.36) immediately brings us

$$R_{SQ} = -\sum_{\boldsymbol{m} \neq \boldsymbol{0}} \lambda_{\boldsymbol{m}} S_{\boldsymbol{m}} Q_{-\boldsymbol{m}}, \tag{3.40}$$

where

$$\lambda_{\boldsymbol{m}} = \frac{\boldsymbol{m} \cdot \hat{\mu}\boldsymbol{f}}{\boldsymbol{m} \cdot \hat{\mu}\boldsymbol{f} - i2\pi \boldsymbol{m} \cdot \hat{\mu}\boldsymbol{m}}, \tag{3.41}$$

Now we can bound the series in (3.40) by treating it as an optimization problem with constraints. But before that let us introduce some properties of $\lambda_{\boldsymbol{m}}$ that becomes handy later in the proof.

Define $\rho_{\boldsymbol{m}}$ to be the real part of $\lambda_{\boldsymbol{m}}$ and $\sigma_{\boldsymbol{m}}$ the imaginary part, so that

$$\lambda_{\boldsymbol{m}} = \rho_{\boldsymbol{m}} + i\sigma_{\boldsymbol{m}}. \tag{3.42}$$

Then

$$\rho_{\boldsymbol{m}}^2 + \sigma_{\boldsymbol{m}}^2 = \rho_{\boldsymbol{m}} = \frac{1}{1 + (\frac{2\pi \boldsymbol{m}\cdot\hat{\mu}\boldsymbol{m}}{\boldsymbol{m}\cdot\hat{\mu}\boldsymbol{f}})^2} \tag{3.43}$$

As we will see later, we need the to find the maximum of $\rho_{\boldsymbol{m}}$ for all $\boldsymbol{m}$. With $\hat{\mu} = \text{diag}(\mu, \mu)$, we can bound $\rho_{\boldsymbol{m}}$ by noting the following relations,

$$\left(\frac{\boldsymbol{m}}{|\boldsymbol{m}|^2}\cdot\boldsymbol{f}\right)^2 \leq \left(\frac{\sum_i |m_i f_i|}{|\boldsymbol{m}|^2}\right)^2 \tag{3.44}$$

$$= \left(\frac{\sum_{i,m_i\neq 0} |f_i/m_i| m_i^2}{|\boldsymbol{m}|^2}\right)^2 \tag{3.45}$$

$$\leq \text{max}_{m_i\neq 0}|f_i/m_i|^2 \tag{3.46}$$

$$\equiv \mathcal{F}^2 \tag{3.47}$$

where $\mathcal{F} = \text{max}_i|f_i|$. The two inequalities holds at the same time when $\boldsymbol{m} \neq \boldsymbol{0}$ satisfies $m_i \in \{1, 0, -1\}$ for $i \in \text{argmax}_j|f_j|$ and $m_i = 0$ otherwise. Plugging in this relation in (3.43) we immediately see

$$\rho_{\boldsymbol{m}} \leq \frac{1}{1 + (2\pi/\mathcal{F})^2},\ \forall \boldsymbol{m} \neq \boldsymbol{0}. \tag{3.48}$$

Now in order to bound (3.40) using optimization, we also need to set up the constraints on S and Q. It turns out to be fruitful to set the constraints on the fluctuations of S and Q, measured by the

variances Var(S) and Var(Q), which can be expressed in Fourier basis as

$$\text{Var}(S) = \sum_{\boldsymbol{m}\neq\boldsymbol{0}} |S_{\boldsymbol{m}}|^2, \tag{3.49}$$

$$\text{Var}(Q) = \sum_{\boldsymbol{m}\neq\boldsymbol{0}} |Q_{\boldsymbol{m}}|^2. \tag{3.50}$$

Before we proceed with the Lagrangian approach, we want to rewrite the expression of R_{SQ} and the variances so that only real, independent variables survive. We note that the R_{SQ} is a real number, so we need to find the real part for the right hand side in (3.40). Let the real parts of $S_{\boldsymbol{m}}$ and $Q_{\boldsymbol{m}}$ be $a_{\boldsymbol{m}}$ and $c_{\boldsymbol{m}}$, respectively, and the imaginary parts of $S_{\boldsymbol{m}}$ and $Q_{\boldsymbol{m}}$ be $b_{\boldsymbol{m}}$ and $d_{\boldsymbol{m}}$, respectively. Because $\lambda_{-\boldsymbol{m}}$, $S_{-\boldsymbol{m}}$ and $Q_{-\boldsymbol{m}}$ are the complex conjugates of $\lambda_{\boldsymbol{m}}$, $S_{\boldsymbol{m}}$ and $Q_{\boldsymbol{m}}$, we know $\rho_{\boldsymbol{m}}$, $a_{\boldsymbol{m}}$ and $c_{\boldsymbol{m}}$ are even in $\boldsymbol{m}$, while $\sigma_{\boldsymbol{m}}$, $b_{\boldsymbol{m}}$ and $d_{\boldsymbol{m}}$ are odd in $\boldsymbol{m}$. Therefore we can rewrite the Lagrangian to reflect this symmetry,

$$L = -2\sum_{\boldsymbol{m}\in\mathcal{M}} \rho_{\boldsymbol{m}}(a_{\boldsymbol{m}}c_{\boldsymbol{m}} + b_{\boldsymbol{m}}d_{\boldsymbol{m}}) + \sigma_{\boldsymbol{m}}(a_{\boldsymbol{m}}d_{\boldsymbol{m}} - b_{\boldsymbol{m}}c_{\boldsymbol{m}}) \tag{3.51}$$

$$-\eta[\text{Var}(S)/2 - \sum_{\boldsymbol{m}\in\mathcal{M}} a_{\boldsymbol{m}}^2 + b_{\boldsymbol{m}}^2] \tag{3.52}$$

$$-\gamma[\text{Var}(Q)/2 - \sum_{\boldsymbol{m}\in\mathcal{M}} c_{\boldsymbol{m}}^2 + d_{\boldsymbol{m}}^2]. \tag{3.53}$$

where the factor 2 comes from the symmetry under flipping the sign of $\boldsymbol{m}$ and $\mathcal{M}$ is the set of independent indices. The optimal response under the constraints has to be the extrema of L, which can be found through the "extrema conditions",

$$\partial_{a_{\boldsymbol{m}}} L = 2(\eta a_{\boldsymbol{m}} - \rho_{\boldsymbol{m}}c_{\boldsymbol{m}} - \sigma_{\boldsymbol{m}}d_{\boldsymbol{m}}) = 0 \tag{3.54}$$

$$\partial_{b_{\boldsymbol{m}}} L = 2(\eta b_{\boldsymbol{m}} + \sigma_{\boldsymbol{m}}c_{\boldsymbol{m}} - \rho_{\boldsymbol{m}}d_{\boldsymbol{m}}) = 0 \tag{3.55}$$

$$\partial_{c_{\boldsymbol{m}}} L = 2(-\rho_{\boldsymbol{m}}a_{\boldsymbol{m}} + \sigma_{\boldsymbol{m}}b_{\boldsymbol{m}} + \gamma c_{\boldsymbol{m}}) = 0 \tag{3.56}$$

$$\partial_{d_{\boldsymbol{m}}} L = 2(-\sigma_{\boldsymbol{m}}a_{\boldsymbol{m}} - \rho_{\boldsymbol{m}}b_{\boldsymbol{m}} + \gamma d_{\boldsymbol{m}}) = 0. \tag{3.57}$$

These are infinite sets of four linear homogeneous equations. To compactly organize them, we define the coefficient matrix

$$M_{\boldsymbol{m}} = \begin{bmatrix} \eta & 0 & -\rho_{\boldsymbol{m}} & -\sigma_{\boldsymbol{m}} \\ 0 & \eta & \sigma_{\boldsymbol{m}} & -\rho_{\boldsymbol{m}} \\ -\rho_{\boldsymbol{m}} & \sigma_{\boldsymbol{m}} & \gamma & 0 \\ -\sigma_{\boldsymbol{m}} & -\rho_{\boldsymbol{m}} & 0 & \gamma \end{bmatrix}.$$

Then the condition for the equations to have nontrivial solutions is

$$\det M_{\boldsymbol{m}} = 0. \tag{3.58}$$

for some $\boldsymbol{m}$, which is equivalent to

$$\rho_{\boldsymbol{m}} = \gamma\eta. \tag{3.59}$$

This condition greatly reduced the number of useful equations in the extrema condition because there will be only a small number of $\boldsymbol{m}$ that can satisfy the above condition. Let $\mathcal{M}_0 \subseteq \mathcal{M}$ the set of $\boldsymbol{m}$ satisfying the above equation and $a_{\boldsymbol{m}}^2 + b_{\boldsymbol{m}}^2 \neq 0$. Assume $\mathcal{M}_0$ is not empty. Then all the terms with $\boldsymbol{m} \notin \mathcal{M}_0$ are eliminated in the series. Next we will evaluate the surviving terms by manipulating the extrema conditions, where all the information about the optimization is encoded. We note that the four extrema conditions are not independent and we actually just need the first two. For all $\boldsymbol{m} \in \mathcal{M}_0$, we multiply (3.54) by $a_{\boldsymbol{m}}$ and (3.55) by $b_{\boldsymbol{m}}$ respectively and manipulate the terms to get

$$\rho_{\boldsymbol{m}} a_{\boldsymbol{m}} c_{\boldsymbol{m}} + \sigma_{\boldsymbol{m}} a_{\boldsymbol{m}} d_{\boldsymbol{m}} = \eta a_{\boldsymbol{m}}^2, \tag{3.60}$$

$$\rho_{\boldsymbol{m}} b_{\boldsymbol{m}} d_{\boldsymbol{m}} - \sigma_{\boldsymbol{m}} b_{\boldsymbol{m}} c_{\boldsymbol{m}} = \eta b_{\boldsymbol{m}}^2. \tag{3.61}$$

Then we manipulate the first two "extrema conditions" so that the term with η is on one side of the

equation, then take the square on both side and sum the two equations to get

$$\eta^2(a_{\boldsymbol{m}}^2 + b_{\boldsymbol{m}}^2) = \rho_{\boldsymbol{m}}(c_{\boldsymbol{m}}^2 + d_{\boldsymbol{m}}^2). \tag{3.62}$$

Since $a_{\boldsymbol{m}}^2 + b_{\boldsymbol{m}}^2 \neq 0$, we get the expression for $|\eta|$,

$$|\eta| = \sqrt{\rho_{\boldsymbol{m}} \frac{c_{\boldsymbol{m}}^2 + d_{\boldsymbol{m}}^2}{a_{\boldsymbol{m}}^2 + b_{\boldsymbol{m}}^2}}. \tag{3.63}$$

Combine (3.60), (3.61), (3.63) with the expression of $|R_{SQ}^{ni}|$ we get

$$|R_{SQ}| = 2 \sum_{\boldsymbol{m} \in \mathcal{M}_0} \sqrt{\rho_{\boldsymbol{m}}(a_{\boldsymbol{m}}^2 + b_{\boldsymbol{m}}^2)(c_{\boldsymbol{m}}^2 + d_{\boldsymbol{m}}^2)}, \tag{3.64}$$

$$\leq \sqrt{\text{Var}(S)\text{Var}(Q) \max_{\boldsymbol{m} \in \mathcal{M}} \rho_{\boldsymbol{m}}}, \tag{3.65}$$

where equality holds in the second equation if $\mathcal{M}_0 = \text{argmax}_{m \in \mathcal{M}} \rho_{\boldsymbol{m}}$. Using (3.48) we immediately arrive at the desired bound.

So we finally conclude that to reach the maximum of $|R_{SQ}|$ under the fixed variances constraints, we need to choose nonuniform S and Q so that they are sinusoidal or uniform in the directions corresponding to $\mathcal{F}$, and uniform in the others. Further, the period of S and Q in $\mathcal{F}$ direction should be 1.

So far we obtained the analytical bound for the response with general mobility perturbation and observable. Now we study the special case, in which $Q(\boldsymbol{r}) = S(\boldsymbol{r}) = \delta_{\mathcal{S}}(\boldsymbol{r})$, as introduced in section 3.2. The proof is quite straightforward. Since $S = Q$, we can plug in $a_{\boldsymbol{m}} = c_{\boldsymbol{m}}$ and $b_{\boldsymbol{m}} = d_{\boldsymbol{m}}$ in the expression of the general perturbation response (3.40) to get the uniform consistent perturbation response

$$R_{\mathcal{S}} = -\sum_{\boldsymbol{m} \neq \boldsymbol{0}} \rho_{\boldsymbol{m}} |S_{\boldsymbol{m}}|^2. \tag{3.66}$$

The variance of S is

$$\mathrm{Var}(S) = \sum_{\boldsymbol{m}\neq\boldsymbol{0}} |S_{\boldsymbol{m}}|^2. \tag{3.67}$$

Therefore we have

$$|R_{\mathcal{S}}| \leq \max_{\boldsymbol{m}\neq\boldsymbol{0}} \rho_{\boldsymbol{m}} \sum_{\boldsymbol{m}\neq\boldsymbol{0}} |S_{\boldsymbol{m}}|^2, \tag{3.68}$$

which immediately leads to the desired bound (3.7). This bound can not be saturated because $\delta_S(\boldsymbol{r})$ has infinite nonzero Fourier components, while the saturation of (3.68) requires a single mode for $S(\boldsymbol{r})$. Our numerics shows that, taking 2D as an example, the optimal perturbation-response region is $[0, 1/2] \times [0, 1]$ for $|f_x| \geq |f_y|$ or $[0, 1] \times [0, 1/2]$ for $|f_x| \leq |f_y|$, together with all the translated regions due to the translational symmetry of the system.

3.5 Discussion

We calculated the average of arbitrary observable due to a general diagonal mobility perturbations for homogeneous nonequilibrium diffusions using Fourier analysis based method. Then we optimized over different perturbation schemes and observables to find the bound on the response. This bound quantitatively characterizes the magnitude of the violation of FDT for such diffusive systems. We could naturally further ask if there is any interesting bound if the mobility matrix is not uniform or diagonal, or if the structure of the perturbation is not the same in different directions. Besides, it is not exactly clear how this bound evolves for a more general drift force $-\nabla U(\boldsymbol{x}) + \boldsymbol{f}$, with $U(\boldsymbol{x})$ being an arbitrary potential landscape. In this case the Fokker-Planck operator $\mathcal{L}$ is no longer diagonal, and clearly we need new tools to address this problem.

CHAPTER 4

Green-Kubo Relation for Active Brownian Particles

This chapter is based on our work published in

[28] Hyun-Myung Chun, Qi Gao, and Jordan M. Horowitz. Nonequilibrium green-kubo relations for hydrodynamic transport from an equilibrium-like fluctuation-response equality. *Phys. Rev. Research*, 3:043172, Dec 2021.

Qi Gao's contribution in this work is to provide numerical simulation and data analysis to verify the Green-Kubo Relations for active Brownian motions.

4.1 Background

At equilibrium, the Green-Kubo relation relates the macroscopic transport coefficient D to the correlation functions of local current $j_{\boldsymbol{r}}(t)$, which depends on location $\boldsymbol{r}$ and time t in a volume V,

$$D\chi = \frac{\beta}{V}\int_0^\infty dt \int_V d\boldsymbol{r} \int_V d\boldsymbol{r}' \langle j_{\boldsymbol{r}}(t) j_{\boldsymbol{r}'}(0)\rangle_{\text{eq}}, \tag{4.1}$$

where χ is the static susceptibility or thermodynamic derivative.

In far-from-equilibrium, as introduced before the FDR allows one to formally link integrals of nonequilibrium correlation functions to microscopic currents [44, 45, 46], in much the same spirit as the macroscopic Green-Kubo relation in (4.1), although this often requires detailed knowledge of the steady state. Nonequilibrium Green-Kubo relations that relate macroscopic transport coef-

ficients to local current observables have appeared in the literature in particular situations. These studies can be categorized according to the method. For a two-dimensional nonequilibrium viscous fluid [47, 48], Green-Kubo relations were deduced by assuming that Onsager's regression hypothesis [49] remains valid around nonequilibrium steady states. An alternative approach utilizes the projection operator method [50, 51] adapted for non-Hamiltonian dynamics [52, 53, 54, 55]. The resulting Green-Kubo relations incorporate a time-reversed dynamics, obscuring the interpretation of the resulting correlation functions. This obstacle has been overcome for at least one specific model of a nonequilibrium active fluid [56].

This chapter is based on our recent work in [28] demonstrating that generally Green-Kubo relations for macroscopic transport coefficients maintain their equilibrium form arbitrarily far from equilibrium by introducing a class of perturbations with explicit conjugate variables whose response is given by simple nonequilibrium correlation functions, akin to the equilibrium FDT. We then exploit this equilibrium-like fluctuation-response equality to provide a theoretical foundation for linearized hydrodynamic equations governing transport in homogenous nonequilibrium fluids. My contribution here is that I provided the numerical support of the Green-Kubo relations theory for the ABPs.

4.2 Theory

In this section we elaborate on the nonequilibrium Green-Kubo relation for the ABPs. We first consider a fluid of N spherical ABPs in a two-dimensional box of size $L \times L$, with periodic boundary conditions. Interactions are modeled through a repulsive, short-ranged, pair potential $\phi(|\boldsymbol{r}_i - \boldsymbol{r}_j|)$. Activity enters by each particle being self-propelled with a velocity $v_0\boldsymbol{e}(\theta_i) = v_0(\cos\theta_i, \sin\theta_i)$, whose orientation θ_i diffuses with diffusion coefficient D_r. Including translational noise with diffusion coefficient D_t leads to an evolution governed by the pair of overdamped Langevin equa-

tions [5, 57]

$$\begin{aligned}\dot{\boldsymbol{r}}_i(t) &= v_0\boldsymbol{e}(\theta_i(t)) + \mu\boldsymbol{F}_i(t) + \sqrt{2D_t}\boldsymbol{\xi}_i(t),\\ \dot{\theta}_i(t) &= \sqrt{2D_r}\eta_i(t),\end{aligned} \tag{4.2}$$

where $\boldsymbol{\xi}_i$ and η_i are independent Gaussian white noises, μ is the bare mobility, and

$$\boldsymbol{F}_i = -\nabla_{\boldsymbol{r}_i}\sum_{j(\neq i)}\phi(|\boldsymbol{r}_i - \boldsymbol{r}_j|) \tag{4.3}$$

is the the total force acting on the i-th particle due to pair interactions. The local particle density is

$$\rho_{\boldsymbol{r}} = \sum_i \delta(\boldsymbol{r} - \boldsymbol{r}_i), \tag{4.4}$$

with Fourier transform

$$\rho_{\boldsymbol{k}} = \sum_i e^{i\boldsymbol{k}\cdot\boldsymbol{r}_i}. \tag{4.5}$$

steady-state average $\bar{\rho} = N/L^2$. The local (density) current is defined as,

$$\boldsymbol{j}_{\boldsymbol{r}} = \sum_i \delta(\boldsymbol{r} - \boldsymbol{r}_i)\dot{\boldsymbol{r}}_i, \tag{4.6}$$

with Fourier transform

$$\boldsymbol{j}_{\boldsymbol{k}} = \sum_i e^{i\boldsymbol{k}\cdot\boldsymbol{r}_i}\dot{\boldsymbol{r}}_i. \tag{4.7}$$

Since the dynamics is symmetric in x and y direction, from now on we only observe the x-directional mode, i.e., $\boldsymbol{k} \propto (2\pi/L, 0)$. Besides, the density transport exhibits an unbiased isotropic diffusion with $\boldsymbol{v} = 0$ and transport coefficient proportional to the identity matrix $\mathsf{D} = D\mathsf{I}$, thus the deviation of $\rho_{\boldsymbol{k}}$ (which we can denote as ρ_k without ambiguity now) from the steady state $\delta\rho_k(t) = \int(\rho_r(t) - \bar{\rho})e^{i\boldsymbol{k}\cdot\boldsymbol{r}}d\boldsymbol{r}$ satisfies by assumption the linear hydrodynamic equation

$$\partial_t\langle\delta\rho_{\boldsymbol{k}}(t)\rangle = -k^2D\langle\delta\rho_{\boldsymbol{k}}(t)\rangle, \tag{4.8}$$

with a diverging relaxation time $\tau(k) = 1/(k^2 D)$.

The nonequilibrium Green-Kubo relation connects the diffusion constant and the correlations between the local density and local currents. For our current setting of ABP system, it can be expressed as

$$D = \frac{\lim_{k\to 0} \int_0^{+\infty} \langle j_k(t+t') j_{-k}(t)\rangle dt' + \lim_{k\to 0} \langle j_k(t)\rho_{-k}(t)\rangle/(ik)}{\lim_{k\to 0}\langle \rho_k(t)\rho_{-k}(t)\rangle}. \tag{4.9}$$

4.3 Simulation

To make a practical simulation, we need to specify more details. Here we use a harmonic interaction potential $\phi(r) = (K/2)(r-a)^2\Theta(a-r)$, with interaction strength K and length a. We use the Euler method to convert the overdamped Langevin equations (4.2) as:

$$\begin{aligned}
x_i[n+1] - x_i[n] &= v_0 \cos(\theta_i[n])\Delta t + \mu F_i^x[n]\Delta t + \sqrt{2D_t\Delta t} G_i^x[n], \\
y_i[n+1] - y_i[n] &= v_0 \cos(\theta_i[n])\Delta t + \mu F_i^y[n]\Delta t + \sqrt{2D_t\Delta t} G_i^y[n], \\
\theta_i[n+1] - \theta_i[n] &= \sqrt{2D_r\Delta t} G_i^\theta[n],
\end{aligned} \tag{4.10}$$

where $G_i^x[n]$, $G_i^y[n]$ and $G_i^\theta[n]$ are independent random numbers subjected to the standard normal distribution.

To numerically verify (4.9), the first step is to measure the "actual" transport coefficient D as the rate of exponential relaxation from an inhomogeneous initial condition per its definition. Then we need to measure the correlation functions in steady state to make "predictions" about D. Finally we need to compare the predictions and the actual results. Therefore there will be two types of simulations and they are different in the following aspects. To measure D directly, we first observed the evolution of the Fourier modes $\rho_{\boldsymbol{k}}$ from a nonuniform initial condition with all the particles uniformly localized to the band $L/4 \le x_i \le 3L/4$, $0 \le y_i \le L$, with $L = 40$ as depicted in Fig.4.1. The time step Δt in this case is chosen to be 0.001 and there are 10^5 steps in total for each simulation. The second simulation is a single long steady-state simulation intended for the

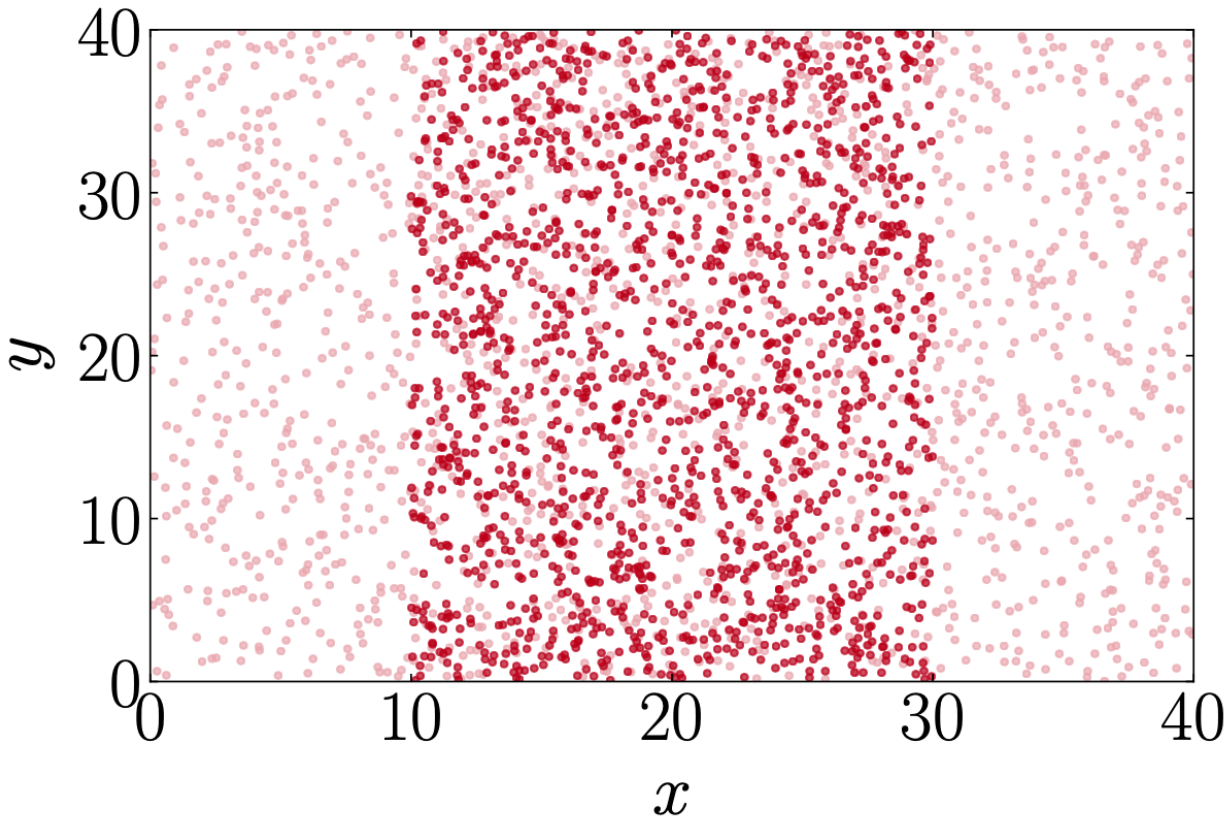

Figure 4.1: Macroscopic relaxation experiment where the particles are initialized to the middle half of the volume (red) and then allowed to evolve in time to a near homogenous configuration (pink).

steady-state correlation functions. We have 400 particles that start from a uniform distribution in the whole $L \times L$ region with $L = 20$. The Δt here is chosen to be 0.005 and 4×10^6 steps are implemented.

And we set $D_t = 0$ to enhance the nonequilibrium effects and facilitate the numerical analysis. As for other parameters, we fix $\mu = 1$,$D_r = 10$ and choose two interaction strength $K = 0.5, 1$ and $v_0 = 1, 2, 3, 4, 5$. For a given parameter set (K, v_0), we perform 10 independent simulations for the relaxation, and 1 simulation for the steady state correlation.

After each simulation, we obtain a data file containing the positions of all the particles at every time step. As a preparation for the data analysis, we are supposed to generate the Fourier density

$\rho_k(t)$ and the x component of the Fourier currents $\boldsymbol{j}_k(t)$, which we shall denote as $j_k(t)$. We have,

$$\rho_{\boldsymbol{k}}[n] = \sum_i e^{ikx_i[n]} \tag{4.11}$$

$$j_k[n] = \sum_i \frac{e^{ikx_i[n]} + e^{ikx_i[n-1]}}{2} \frac{x_i[n] - x_i[n-1]}{\Delta t} \tag{4.12}$$

Now we start to calculate D from relaxations. Each mode $\rho_k(t)$ decays exponentially in time for with an exponent $-1/\tau(k)$. In practice, due to the increasing noise (see Fig. 4.2) in the higher-mode data we only use the lowest mode $k_{\min} = 2\pi/L$ to obtain the corresponding $1/\tau$, then estimate D from $\tau/(2\pi/L)^2$. Taking the average and standard error on the mean over ten independently measured D, we estimate the transport coefficient and its error. We then repeat the above for all the ten parameter combinations.

Next we need to predict D from correlation functions. We have three correlation terms to evaluate,

$$\tilde{\chi} = \lim_{k\to 0} \langle \rho_k(t)\rho_{-k}(t)\rangle \tag{4.13}$$

$$C = \lim_{k\to 0} \int_0^{+\infty} \langle j_k(t+t')j_{-k}(t)\rangle dt' \tag{4.14}$$

$$E = \lim_{k\to 0} \frac{\langle j_k(t)\rho_{-k}(t)\rangle}{ik}. \tag{4.15}$$

The averages are taken over steady states so we drop the first 8×10^5 data points in $\rho_k(t)$, $j_k(t)$ and checked that $\rho_k(t)$ is roughly in the steady state. When dealing with the limit of $k\to 0$ in (4.13), although we are aware that we could evaluate those correlations with several k and take the extrapolation, be it linear or quadratic, we realize that this approach may not always be the most reasonable due to the presence of increasing noise as k becomes higher, as we can see from Fig. 4.2. Therefore, instead of taking the extrapolation, we use the smallest $k = k_{\min} = 2\pi/L$ as an approximate. In (4.14), the limit and the integral commute, authorizing us to plug in j_0. In (4.15), the numerator is supposed to be zero in the $k\to 0$ limit and we are concerned of the slope of the imaginary part of $\langle j_k(t)\rho_{-k}(t)\rangle$ as a function of k as $k\to 0$. Again due to the noise and the

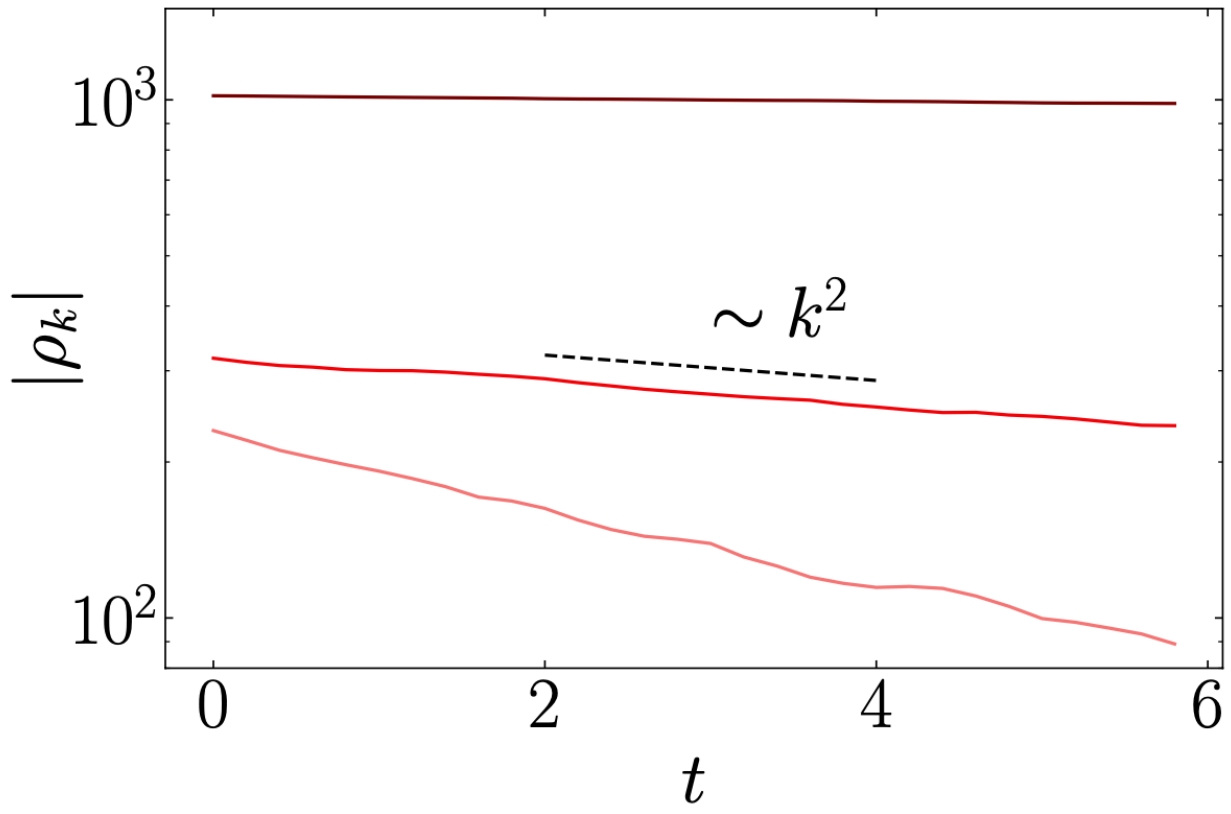

Figure 4.2: The first three non-zero Fourier modes in the x-direction $|\rho_k|$ with $k \in \{2\pi/L, 6\pi/L, 10\pi/L\}$ (from top to bottom) display the expected exponential relaxation with a k-dependent slope confirming the hydrodynamic behavior.

nonlinearity as k increases, we decide to approximate this slope using that of the two smallest k, namely k_{min} and $2k_{min}$. To be precise mathematically, we are actually evaluating

$$\hat{\tilde{\chi}} = \langle \rho_{k_{\min}}(t)\rho_{-k_{\min}}(t)\rangle \tag{4.16}$$

$$\hat{C} = \int_0^{+\infty} \langle j_0(t+t')j_0(t)\rangle dt' \tag{4.17}$$

$$\hat{E} = \frac{\mathrm{Im}(\langle j_{2k_{\min}}(t)\rho_{-2k_{\min}}(t)\rangle - \langle j_{k_{\min}}(t)\rho_{-k_{\min}}(t)\rangle)}{k_{\min}}. \tag{4.18}$$

The evaluation of (4.16) is straightforward. We simply compute

$$\sum_n |\rho_{k_{\min}}[n]|^2 . \tag{4.19}$$

For (4.17), we want first to evaluate the integrand, which the a autocorrelation of $j_0(t)$ with lag t'. There are several possible ways to deal with it. Here we use the discrete Wiener-Khinchin Theorem to compute the correlation from the power spectrum. For continuous function $a(t)$ and $b(t)$ with respectively corresponding discrete data arrays $A[n]$ and $B[n]$ this is phrased as

$$\langle a(t+t')b(t)\rangle = \lim_{N\to\infty} \frac{1}{N^2} \sum_{p=0}^{N-1} e^{2\pi ipn/N} \tilde{A}[p]\tilde{B}^*[p], \tag{4.20}$$

where n denotes the nth entry in the correlation function array. $\tilde{B}^*[p]$ is the complex conjugate of $\tilde{B}[p]$. The Fourier transform here for $A[n]$ follows the definition of the fast Fourier transform function in Python

$$\tilde{A}[p] = \sum_{n=0}^{N-1} e^{-2\pi ipn/N} A[n]. \tag{4.21}$$

The same applies to $\tilde{B}[p]$. Since the N we use is large, we approximate the limit of $N \to \infty$ with this finite N. And we let $a(t) = b(t) = j_0(t)$ to get the approximation for $\langle j_0(t+t')j_0(t)\rangle$. Assuming that the correlation function decreases exponentially in t', we can evaluate the integral in (4.17) as

$$\frac{\frac{1}{N^2}\sum_{p=0}^{N-1} \left|\tilde{j}_0[p]\right|^2}{-K}. \tag{4.22}$$

where $\tilde{j}_0[p]$ follows the definition of the Fourier transform above and K is the slope in the linear fit of $\ln|\langle a(t+t')b(t)\rangle|$ versus t'.

Similarly, for (4.18) we use the Wiener-Khinchin Theorem to evaluate the cross correlation function by substituting $A[n]$ with $j_{2k_{\min}}[n]$ or $j_{2k_{\min}}[n]$ and $B[n]$ with $\rho_{-2k_{\min}}[n]$ or $\rho_{-2k_{\min}}[n]$.

To analyze the error, we divide $\rho_k[n]$ and $j_k[n]$ into 10 blocks and repeat the above procedure for each block of data to get D_i. Then we take the average and the error of the mean to get our final result as well as the error.

Before we show the numerical plots, we complement the numerical validation with an analytic

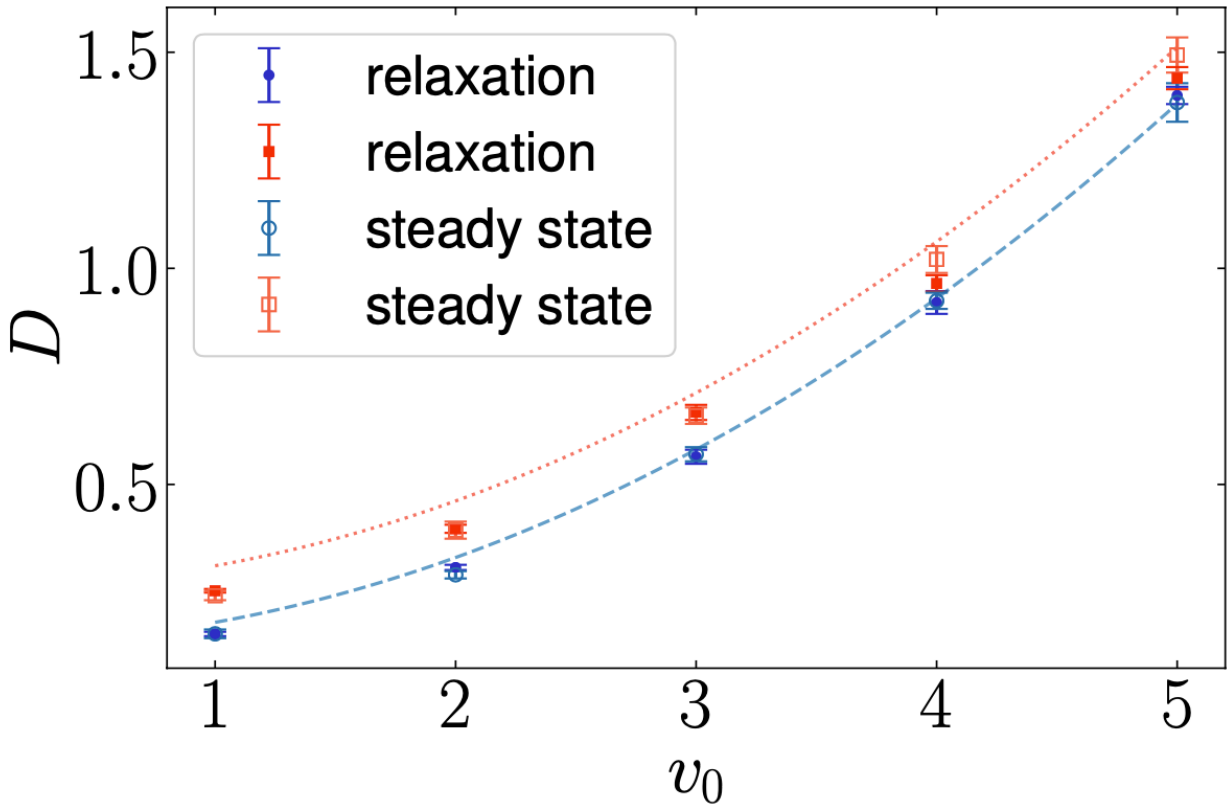

Figure 4.3: Comparison of the transport coefficient measured using the macroscopic relaxation method (filled symbols) to the prediction of the Green-Kubo relation (4.9) obtained from steady-state correlation functions (open symbols) as a function of activity v_0 for two interaction strengths, $K = 0.5$ (blue), and $K = 1.0$ (red). The dashed ($K = 0.5$) and dotted ($K = 1.0$) lines are analytic predictions from the linear theory.

analysis to gain further insight. The microscopic dynamics of the density ρ_r is given by a nonlinear stochastic differential equation with multiplicative noise, known as the Dean equation [58, 59].

Following [59], in [28] we derived a linear Gaussian dynamics that can be solved analytically allowing us to determine each term in the Green-Kubo relation, which are

$$\begin{aligned} \tilde{\chi} &= \frac{N[D_t + v_0^2/(2D_r)]}{D_t + \mu\bar{\rho}\phi_0 + v_0^2/(2D_r)}, \\ C &= \frac{Nv_0^2}{2D_r}, \\ E &= ND_t, \end{aligned} \tag{4.23}$$

where $\phi_0 = \lim_{k\to 0} \phi_{\boldsymbol{k}}$ is the zero wave-vector limit of the pair potential. Combining, we arrive at a prediction for the transport coefficient

$$D = D_t + \mu\bar{\rho}\phi_0 + \frac{v_0^2}{2D_r}. \tag{4.24}$$

The second term on the right hand side is the correction from the interaction of particles. For repulsive interactions, this term is positive and proportional to the mobility, the average density and the strength of the interaction. The third term is the correction due to the particles being active. It increases with the self-propelling speed v_0 and decrease with the diffusion coefficient D_r of the orientation. The predictions from this linearized theory (4.24) are compared to the simulation in Fig. 4.3 where the dashed line is for the weaker interaction ($K = 0.5$) and the dotted is the stronger interaction ($K = 1.0$). For the weaker interaction ($K = 0.5$), the linear approximation agrees well with the simulations when v_0 is large. When v_0 is small, the predictions of the linear theory for both the strong and weak interactions fall outside the error bars, overestimating the transport coefficient. Even still, the coincidence of the two numerical measurements of D suggests the macroscopic Green-Kubo relation remains valid.

CHAPTER 5

Summary

5.1 Constraints on Responses in Diffusion

The responses in average of observables can be conveniently related to the correlations of the observable and the conjugate variable at equilibrium through FDT. At far-from-equilibrium, FDR gives similar relations but the conjugate variable is in general unknown since it requires the exact knowledge of the probability distribution. The contribution of this thesis is that it serves as part of a whole different framework, where we study the bound on the responses for all possible distributions, regardless of the exact form of it. In chapter 2, we proposed a complete parameterization for a general one dimensional diffusion process Eq. (1.31), so that we can study responses for each parameter separately. Borrowing language from a colloidal particle in a viscous fluid, we denote the parameters as "mobility" μ, potential "energy" U and constant driving "force" f. We found that the responses due to a combination of the mobility and energy perturbation satisfies an equilibrium-like FDT Eq. (2.6). The response due to the mobility perturbation, which notably has the physical meaning of the violation of the FDT, is bounded by how far the system is out of equilibrium, Eq. (2.7) and Eq. (2.9). Finally the bound on the force perturbation is shown in Eq. (2.8) and Eq. (2.10).

Analysis of the responses in the 1D diffusions naturally motivates us to explore higher dimensions. Specifically, we noticed that the mobility perturbation is a nonequilibrium effect and we want to study it for higher dimensions. Without a full closed-form solution to the FPE in dimen-

sions higher than one, we can use the Fourier expansion method introduced in section 3.3 to make progress. To derive the bound analytically, we focus on a simpler classes of model with driven diffusions in a flat energy landscape. For such system the system parameters are fixed so we maximized over all observables and conjugate variables. We found that the response for a general obseravable and a range of mobility perturbation scheme is bounded by their variations and how far the system is out of equilibrium in Eq. (3.6). If we increase the restrictions by requiring the observable and the conjugate variable to be the same indicator functions, we can prove a tighter analytical bound Eq. (3.7) on the mobility perturbation response. This bound however can not be saturated. Numerical study shows that such responses share a same bound for arbitrary dimensions, which suggests the analytical form of this bound can be derived by considering the responses in 1D diffusions, as is shown in Eq. (3.8).

Possible future work includes the generalization of the bounds for more general models in higher dimension where the potential landscape is not flat and the mobility matrix being non-diagonal and anisotropic. Analysis of such systems may require novel methodologies. Besides, it is possible that all of these results could also be translated to quantum systems, if we can set up the correspondence between the classical diffusion model and the quantum system properly, although the details of this hypothesis requires a careful and thorough inspection. In addition, it is interesting to ask if we can perform similar analysis for non-static perturbation responses, which may provide insights in a broader context. For example in biochemical oscillations [60], the energy dissipation rate is related to the correlation of the peak phases of oscillations, and a study on non-static perturbation responses could lead to such correlations too.

5.2 Green-Kubo Relation for Active Brownian Particles

At equilibrium, the Green-Kubo relation relates the diffusion coefficients to the correlations of local currents. In far-from-equilibrium, similar relations also appeared in particular situations. For the ABP system, our recent work developed the Green-Kubo relations Eq. (4.9). Such prediction

was numerically verified using molecular dynamics simulations and data analysis in chapter 4. Our analysis is valid for any Markovian system with statistically translationally invariant steady state. So it is an interesting question to ask if relaxing the Markovian assumption may be possible, since non-Markovian dynamics can be made Markovian by introducing auxiliary variables [61]. Other possible future work includes the study of inhomogeneous boundary driven steady states, when the environmental interactions can be modeled via Markovian stochastic processes.

BIBLIOGRAPHY

[1] R. Kubo, M. Toda, and N. Hashitsume. *Statistical Physics II: Nonequilibrium Statistical Mechanics*. Springer-Verlag, Berlin, 1985.

[2] L. P. Kadanoff and P. Martin. Hydrodynamic equations and correlation functions. *Ann. Phys.*, 24:419–469, 1963.

[3] D. Forster. *Hydrodynamic fluctuations, broken symmetry, and correlation functions*. W. A. Benjamin, Inc., Reading, Massachusetts, 1975.

[4] P. M. Chaikin and T. C. Lubensky. *Principles of Condensed Matter Physics*. Cambridge University Press, 1995.

[5] Y. Fily and M. C. Marchetti. Athermal phase separation of self-propelled particles with no alignment. *Phys. Rev. Lett.*, 108:235702, 2012.

[6] J. Bialké, H. Löwen, and T. Speck. Microscopic theory for the phase seperation of self-propelled repulsive disks. *Europhys. Lett.*, 103(3):30008, 2013.

[7] P. Martin, A. J. Hudspeth, and F. Jülicher. Comparison of a hair bundle's spontaneous oscillations with its response to mechanical stimulation reveals the underlying active process. *Proc. Natl. Acad. Sci. USA*, 98(25):14380–14385, 2001.

[8] Daisuke Mizuno, Catherine Tardin, C. F. Schmidt, and F. C. MacKintosh. Nonequilibrium mechanics of active cytoskeletal networks. *Science*, 315(5810):370–373, 2007.

[9] K. Sato, Y. Ito, T. Yomo, and K. Kaneko. On the relation between fluctaution and response in biological systems. *Proc. Natl. Acad. Sci. USA*, 100:14086, 2003.

[10] A. Murugan, D. A. Huse, and S. Leibler. Speed, dissipation, and error in kinetic proofreading. *Proc. Natl. Acad. Sci. USA*, 109:12034–12039, 2011.

[11] H. Qian. Coopertivity in cellular biochemical processes: Noise-enhanced sensitivity, fluctuating enzyme, bistability with nonlinear feedback, and other mechanisms for sigmoidal responses. *Ann. Rev. Biophys.*, 41:179–204, 2012.

[12] C.-C. S. Yan and C.-P. Hsu. The fluctuation-dissipation theorem for stochastic kinetics - implications on genetic regulations. *J. Chem. Phys.*, 139:224109, 2013.

[13] D. Hartich, A. C. Barato, and U. Seifert. Nonequilibrium sensing and its analogy to kinetic proofreading. *New J. Phys.*, 17:055026, 2015.

[14] J. Estrada, F. Wong, A. DePace, and J. Gunawardena. Information integration and energy expenditure in gene regulation. *Cell*, 166:234–244, 2016.

[15] G. S. Agarwal. Fluctuation-dissipation theorems for systems in non-thermal equilibrium and applications. *Z. Phys. A*, 252:25–38, 1972.

[16] J. Prost, J.-F. Joanny, and J. M. R. Parrondo. Generalized fluctuation-dissipation theorem for steady-state systems. *Phys. Rev. Lett.*, 103:090601, Aug 2009.

[17] E. Ben-Isaac, Y. K. Park, G. Popescu, F. L. H. Brown, N. S. Gov, and Y. Shokef. Effective temperature of red-blood-cell membrane fluctuations. *Phys. Rev. Lett.*, 106:238103, 2011.

[18] Leticia F Cugliandolo. The effective temperature. *Journal of Physics A: Mathematical and Theoretical*, 44(48):483001, nov 2011.

[19] E. Dieterich, J. Camunas-Soler, M. Ribezzi-Crivellari, U. Seifert, and F. Ritort. Single-molecule measurement of the effective temperature in non-equilibrium steady states. *Nat. Phys.*, 11:971–977, 2015.

[20] Takahiro Harada and Shin-ichi Sasa. Equality connecting energy dissipation with a violation of the fluctuation-response relation. *Phys. Rev. Lett.*, 95:130602, Sep 2005.

[21] S. Toyabe, T. Okamoto, T. Watanabe-Nakayama, H. Taketani, S. Kudo, and E. Muneyuki. Nonequilibrium energetics of a single f_1-atpase molecule. *Phys. Rev. Lett.*, 104:198103, 2010.

[22] Todd R. Gingrich, Jordan M. Horowitz, Nikolay Perunov, and Jeremy L. England. Dissipation bounds all steady-state current fluctuations. *Phys. Rev. Lett.*, 116:120601, Mar 2016.

[23] Todd R Gingrich, Grant M Rotskoff, and Jordan M Horowitz. Inferring dissipation from current fluctuations. *Journal of Physics A: Mathematical and Theoretical*, 50(18):184004, apr 2017.

[24] Jordan M. Horowitz and Todd R. Gingrich. Thermodynamic uncertainty relations constrain non-equilibrium fluctuations. *Nature Physics*, 2019.

[25] Junang Li, Jordan M. Horowitz, Todd R. Gingrich, and Nikta Fakhri. Quantifying dissipation using fluctuating currents. *Nature Communications*, 10(1):1666, 2019.

[26] Patrick Pietzonka, Andre C Barato, and Udo Seifert. Universal bound on the efficiency of molecular motors. *Journal of Statistical Mechanics: Theory and Experiment*, 2016(12):124004, dec 2016.

[27] Jeremy A. Owen, Todd R. Gingrich, and Jordan M. Horowitz. Universal thermodynamic bounds on nonequilibrium response with biochemical applications, 2019.

[28] Hyun-Myung Chun, Qi Gao, and Jordan M. Horowitz. Nonequilibrium green-kubo relations for hydrodynamic transport from an equilibrium-like fluctuation-response equality. *Phys. Rev. Research*, 3:043172, Dec 2021.

[29] L. Peliti and S. Pigolotti. *Stochastic Thermodynamics: An Introduction*. Princeton University Press, 2021.

[30] Alex J. Levine and T. C. Lubensky. One- and two-particle microrheology. *Phys. Rev. Lett.*, 85:1774–1777, Aug 2000.

[31] Jakob Mehl, Valentin Blickle, Udo Seifert, and Clemens Bechinger. Experimental accessibility of generalized fluctuation-dissipation relations for nonequilibrium steady states. *Phys. Rev. E*, 82:032401, Sep 2010.

[32] M. Baiesi, C. Maes, and B. Wynants. Fluctuations and response in nonequilibrium states. *Phys. Rev. Lett.*, 103:010602, 2009.

[33] Seifert, U. and Speck, T. Fluctuation-dissipation theorem in nonequilibrium steady states. *EPL*, 89(1):10007, 2010.

[34] David K. Lubensky. Equilibriumlike behavior in chemical reaction networks far from equilibrium. *Phys. Rev. E*, 81:060102, Jun 2010.

[35] Bernhard Altaner, Matteo Polettini, and Massimiliano Esposito. Fluctuation-dissipation relations far from equilibrium. *Phys. Rev. Lett.*, 117:180601, Oct 2016.

[36] J. R. Gomez-Solano, A. Petrosyan, S. Ciliberto, R. Chetrite, and K. Gawedzki. Experimental verification of a modified fluctuation-dissipation relation for a micron-sized particle in a nonequilibrium steady state. *Phys. Rev. Lett.*, 103:040601, Jul 2009.

[37] Takahiro Ohkuma and Takao Ohta. Fluctuation theorems for non-linear generalized langevin systems. *Journal of Statistical Mechanics: Theory and Experiment*, 2007(10):P10010, oct 2007.

[38] Takahiro Harada. Macroscopic expression connecting the rate of energy dissipation with the violation of the fluctuation response relation. *Phys. Rev. E*, 79:030106, Mar 2009.

[39] Takahiro Harada and Shin-ichi Sasa. Energy dissipation and violation of the fluctuation-response relation in nonequilibrium langevin systems. *Phys. Rev. E*, 73:026131, Feb 2006.

[40] C. W. Gardiner. *Handbook of Stochastic Methods for Physics, Chemistry and the Natural Sciences*. Springer-Verlag, New York, 3rd edition, 2004.

[41] Qi Gao, Hyun-Myung Chun, and Jordan M. Horowitz. Thermodynamic constraints on the nonequilibrium response of one-dimensional diffusions. *Phys. Rev. E*, 105:L012102, Jan 2022.

[42] R. Graham. Covariant formulation of non-equilibrium statistical thermodynamics. *Z. Physik B*, 26:397–405, 1977.

[43] Jeremy A. Owen, Todd R. Gingrich, and Jordan M. Horowitz. Universal thermodynamic bounds on nonequilibrium response with biochemical applications. *Phys. Rev. X*, 10:011066, Mar 2020.

[44] Udo Seifert. Generalized einstein or green-kubo relations for active biomolecular transport. *Phys. Rev. Lett.*, 104(13):138101, 2010.

[45] Kiryl Asheichyk, Alexandre P Solon, Christian M Rohwer, and Matthias Krüger. Response of active brownian particles to shear flow. *J. Chem. Phys.*, 150(14):144111, 2019.

[46] Sara Dal Cengio, Demian Levis, and Ignacio Pagonabarraga. Linear response theory and green-kubo relations for active matter. *Phys. Rev. Lett.*, 123(23):238003, 2019.

[47] Jeffrey M Epstein and Kranthi K Mandadapu. Time-reversal symmetry breaking in two-dimensional nonequilibrium viscous fluids. *Phys. Rev. E*, 101(5):052614, 2020.

[48] Cory Hargus, Katherine Klymko, Jeffrey M Epstein, and Kranthi K Mandadapu. Time reversal symmetry breaking and odd viscosity in active fluids: Green–kubo and nemd results. *J. Chem. Phys.*, 152(20):201102, 2020.

[49] Lars Onsager. Reciprocal relations in irreversible processes. i. *Phys. Rev.*, 37(4):405, 1931.

[50] Hazime Mori. Transport, collective motion, and brownian motion. *Prog. Theor. Phys.*, 33(3):423–455, 1965.

[51] Robert Zwanzig. *Nonequilibrium statistical mechanics*. Oxford University Press, 2001.

[52] MH Ernst and Ricardo Brito. Generalized green-kubo formulas for fluids with impulsive, dissipative, stochastic, and conservative interactions. *Phys. Rev. E*, 72(6):061102, 2005.

[53] MH Ernst and Ricardo Brito. New green-kubo formulas for transport coefficients in hard-sphere, langevin fluids and the likes. *Europhys. Lett.*, 73(2):183, 2005.

[54] Pep Español. Coarse graining from coarse-grained descriptions. *Philos. Trans. A: Math. Phys. Eng. Sci.*, 360(1792):383–394, 2002.

[55] Pep Español. Einstein-helfand form for transport coefficients from coarse-grained descriptions. *Phys. Rev. E*, 80(6):061113, 2009.

[56] Ming Han, Michel Fruchart, Colin Scheibner, Suriyanarayanan Vaikuntanathan, William Irvine, Juan de Pablo, and Vincenzo Vitelli. Statistical mechanics of a chiral active fluid. *arXiv*, February 2020.

[57] Julian Bialké, Thomas Speck, and Hartmut Löwen. Crystallization in a dense suspension of self-propelled particles. *Phys. Rev. Lett.*, 108(16):168301, 2012.

[58] David S Dean. Langevin equation for the density of a system of interacting langevin processes. *J. Phys. A: Math. Gen.*, 29(24):L613, 1996.

[59] Vincent Démery, Olivier Bénichou, and Hugo Jacquin. Generalized langevin equations for a driven tracer in dense soft colloids: construction and applications. *New J. Phys.*, 16(5):053032, 2014.

[60] Yuansheng Cao, Hongli Wang, Qi Ouyang, and Yuhai Tu. The free-energy cost of accurate biochemical oscillations. *Nature Physics*, 11(9):772–778, 2015.

[61] H. Risken. *The Fokker-Planck Equation: Methods of Solution and Applications*. Springer-Verlag, New York, 1984.